



Original Paper

Hydrocarbon Generation Potential of the Organic-Rich Naifa Formation, Say'un–Masila Rift Basin, Yemen: Insights from Geochemical and Palynofacies Analyses

Mohammed Hail Hakimi,^{1,2} Wan Hasiah Abdullah,¹ Aref A. Lashin ,^{3,6} El-Khedr H. Ibrahim,⁴ and Yousif M. Makeen⁵

Received 2 April 2019; accepted 18 November 2019
Published online: 27 November 2019

The Say'un–Masila rift, one of the most important basins of Yemen, contains unconventional resources of organic-rich rocks. In the present work, geochemical and palynofacies analyses were performed on the organic-rich source rock (argillaceous limestone) of the late Jurassic–early Cretaceous Naifa Formation in the Say'un–Masila Rift Basin to investigate its hydrocarbon generation potential. The geochemical analysis of the organic matter reveals that the argillaceous limestone unit has total organic carbon contents of 0.5–2.6%, which indicate fair to good hydrocarbon source potential. The organic matter in the analyzed samples is dominated by Type II/III and Type III kerogens, with minor Type II kerogen, referring to both oil- and gas-prone source rocks. The dominant kerogen Types II/III and Type III are indicated further from quantitative results based on an open pyrolysis–gas chromatography analysis. Biological markers and palynofacies analysis suggest that the kerogen was formed through a combination of mixed marine and high land plant organic matter and was preserved under sub-oxic sedimentary conditions. The different geochemical and optical maturity parameters indicate that the analyzed argillaceous limestone of the Naifa Formation is thermally mature, equivalent to early mature of oil-generation window. This implies that the burial depth of the analyzed samples is not deep enough; therefore, only the deeper parts of the Naifa source rocks at the basin have reached a satisfactory maturity level to be considered as potentially effective petroleum source rock. The biomarker source and depositional environment indicators presented and discussed in this study are useful for future exploration in the Say'un–Masila Basin for oil-to-oil and oil-to-source geochemical correlations and offer guidance for potential prospecting targets that may occur within the basin.

KEY WORDS: Naifa Formation, Organic-rich argillaceous limestone, Geochemical analyses, Palynofacies, Hydrocarbon potential, Say'un–Masila Basin—Yemen.

¹Geology Department, University of Malaya, 50603 Kuala Lumpur, Malaysia.

²Geology Department, Faculty of Applied Science, Taiz University, 6803 Taiz, Yemen.

³Petroleum and Natural Gas Engineering Department, College of Engineering, King Saud University, PO Box 800 Riyadh 11421, Saudi Arabia.

⁴Department of Geology and Geophysics, College of Science, King Saud University, PO Box 2455 Riyadh 11451, Saudi Arabia.

⁵College of Earth Sciences, Jilin University, Changchun 130061, China.

⁶To whom correspondence should be addressed; e-mail: ar-lashin@ksu.edu.sa

INTRODUCTION

This study was conducted on sedimentary rocks exposed in the west central portion of the Say'un–Masila Rift Basin (Fig. 1a). This basin is located at the eastern province of Yemen. It is a highly promising target for hydrocarbon exploration and development (Fig. 1a). The Mesozoic sedimentary succession in the Masila Basin of Yemen is a prime target for new petroleum discoveries by many oil companies (Fig. 1b). It comprises many stratigraphic layers with many unconventional resources and good source rock characteristics (Madbi, Naifa and Saar Formations). The Late Jurassic Madbi Formation is regionally exposed throughout the Say'un–Masila Basin and has been subjected to extensive investigations and identified to be a major source rock in the area (Hakimi et al. 2010b, 2011, 2012a;

Al Areeq et al. 2011; Bawazer et al. 2018). However, little has been reported on the evolution of the younger Mesozoic sedimentary successions in the Say'un–Masila Basin (i.e., the Naifa and Saar Formations) in terms of organic facies richness, thermal maturity, and sedimentary conditions, in relation to the hydrocarbon generation potential.

In the present study, the younger Mesozoic deposits of the Naifa Formation are investigated using geochemical and optical methods. The main aim was to evaluate the source rock potential of this formation by determining its organic matter type/richness, thermal maturity and type of possible generated hydrocarbons. Although mainly used for determining the source rock potential in the studied formation, the biomarker and palynofacies data also provided information regarding the organic matter sources (marine, lacustrine, terrestrial) and paleo-

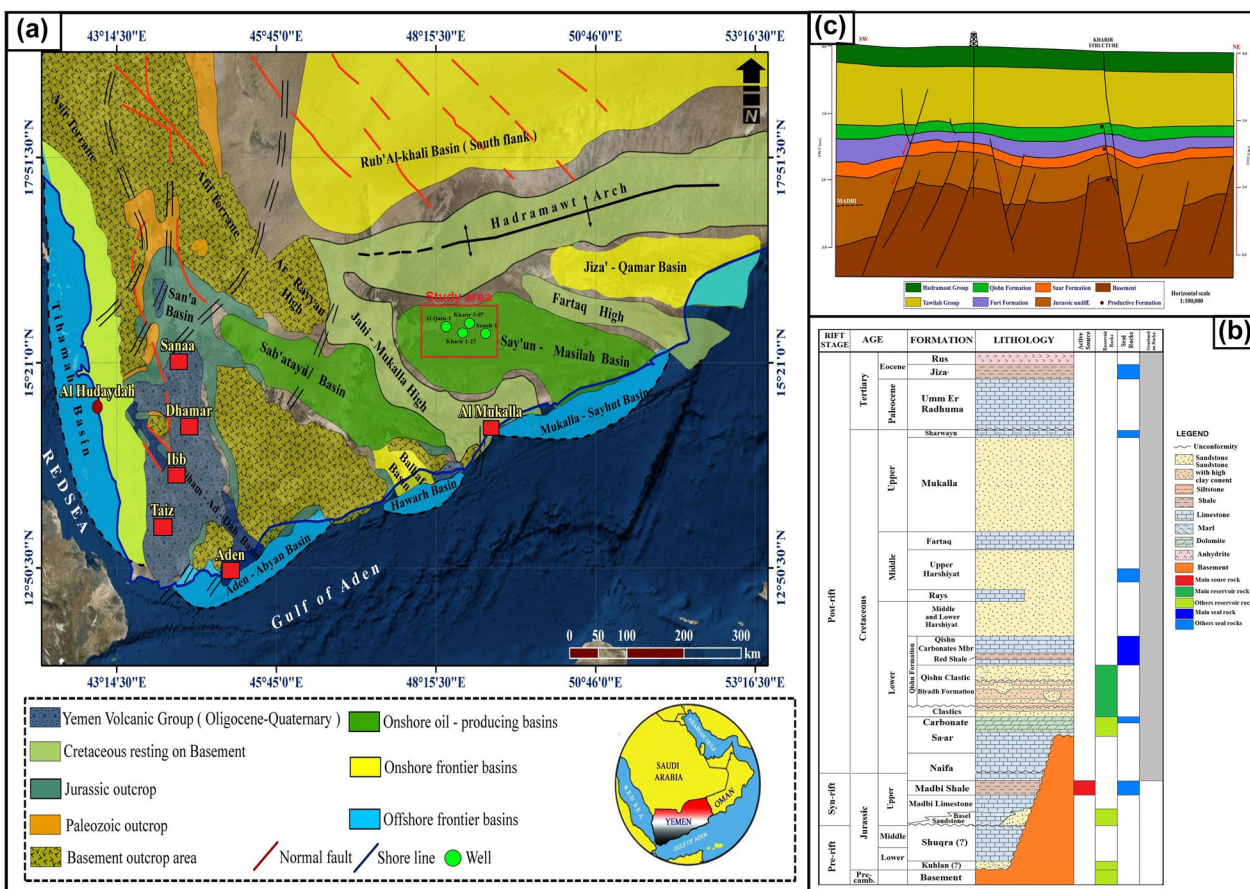


Figure 1. (a) Map of main sedimentary basins in the Republic of Yemen (modified after Beydoun et al. 1998) showing locations of the study area and the studied wells. (b) Regional stratigraphy of the Say'un–Masila Basin, Eastern Yemen (compiled from Hakimi et al. 2011). (c) Structural cross section across Kharir oilfields, showing the main structural types in the Say'un–Masila Basin (modified after SPT 1994).

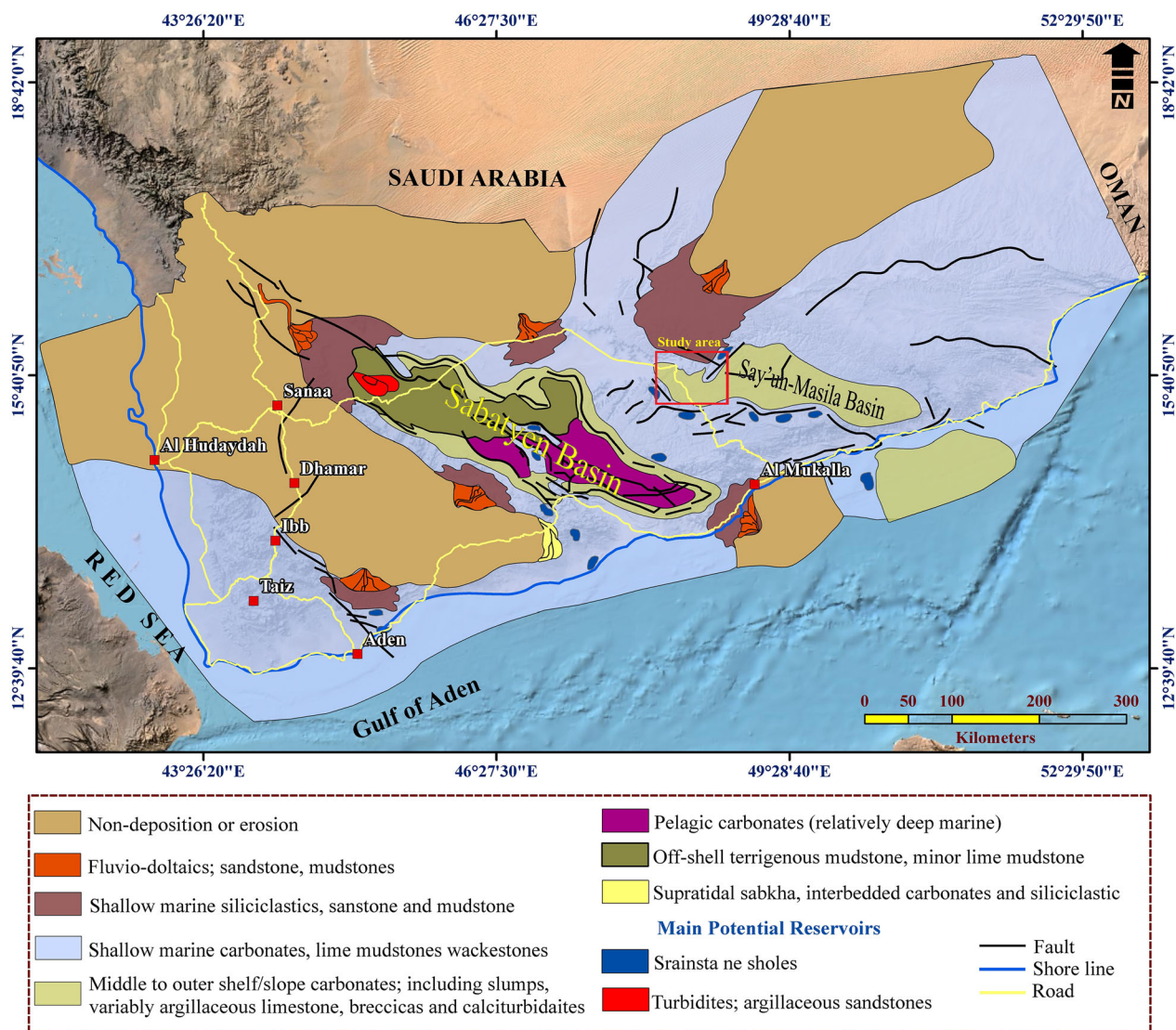


Figure 2. Map view of palynofacies during the late Jurassic to early the Cretaceous for the Naifa Formation in the sedimentary basins of Yemen (modified after SPT 1994).

depositional conditions, in terms of oxygenation levels (e.g., anoxic vs. oxic). The outcomes of this study enhance our current knowledge and understanding of the basin for better prediction of new source rock targets, which would be beneficial to further hydrocarbon exploration activities in the basin.

GEOLOGICAL SETTING

Yemen includes numerous offshore and onshore sedimentary basins (Fig. 1a), which are related

to and generated mainly by plate tectonics activities that began at the end of the Jurassic and beginning of the Cretaceous when southern Gondwana broke apart and continued into the Oligocene–Miocene with the formations of the Gulf of Aden and the Red Sea (Redfern and Jones 1995; Beydoun et al. 1998; Csato et al. 2001).

The Say'un–Masila Basin is an onshore rift basin. It occupies the east central province of Yemen in the Hadhramaut region (Fig. 1a) and is associated with the Mesozoic disintegration of Gondwana (Redfern and Jones 1995). The initial rifting event occurred during the end of Jurassic and accelerated

into the beginning of Cretaceous. This was followed by intermittent rifting and sagging of the basin along with sea level incursions and withdrawals (Redfern and Jones 1995). These tectonic rifting events are manifested by several normal faults and are associated with many structural highs (horsts), lows (grabens), and tilted blocks (Fig. 1c), which are considered to be major structural bodies for hydrocarbon trapping (King et al. 2003; Hakimi et al. 2012b). The filling of the basin began in Jurassic and continued until the Tertiary and resulted in deposition of a thick sedimentary succession that was controlled by the interplay of both tectonic activities and sea level fluctuation (Fig. 1b).

The Jurassic units are represented mostly by continental to marine deposits of the Kuhlan Formation, which overlies unconformably the Precambrian basement rocks (Fig. 1b). The composition of Kuhlan Formation is mainly fluvial arkosic sandstone, which grades vertically into a shallow-marine carbonate series (Shuqra Formation) (Beydoun et al. 1998; Al-Wosabi and Al-Mashaikie 2006). The Late Jurassic Shuqra Formation underlies conformably the Madbi Formation and consists of fossiliferous marl-dominated neritic carbonate deposits (Beydoun et al. 1998) (Fig. 1b). During late Jurassic, commencing in the Kimmeridgian, renewal of tectonic uplifting of the basin flanks accompanied by sagging of the basin and relative sea level rise resulted in a new cycle of sedimentation beginning with the basal sandstone facies of the Madbi Formation followed by relatively deeper carbonates and shale facies (Beydoun et al. 1998). According to recent geochemical investigations in the basin, the upper part of the Madbi Formation is composed of organic-rich shale that is mainly oil-generating, and marine in origin (Mills 1992; Hakimi et al. 2010a, b, 2011; Al Areeq et al. 2011; Al Areeq and Maky 2015; Hakimi et al. 2016). A mixed carbonate and shale marine sequence of the Naifa Formation was deposited during the latest Jurassic–earliest Cretaceous (Beydoun 1964; Beydoun et al. 1998). The Naifa Formation is exposed mainly in the onshore and offshore basins of Yemen and is composed of mainly carbonates and siliciclastics such as calcareous shale, shale and claystone inter-beds in the type locality of Hajar Trough (SPT 1994; Beydoun et al. 1998; Fig. 2). These rocks reflect shallow marine, pelagic rift to open marine conditions (SPT 1994; Beydoun et al. 1998). In the Say'un–Masila Basin, the Naifa Formation is mainly composed of middle to outer shelf/slope carbonate rocks including lime

mudstones, wackestones, and variably argillaceous limestones (SPT 1994; Fig. 2). The Naifa Formation is conformably overlain by the post-rift series beginning with the Early Cretaceous (Valanginian) Saar Formation (Fig. 1b). This post-rift series is overlain unconformably by syn-rift deposits and is composed of Cretaceous and Tertiary clastic and carbonate rocks of the Saar Formation with evaporates of the Rus Formation (Fig. 1b). The major reservoir rocks are represented by the clastics of the Kuhlan, Madbi and Qishn Formations and the carbonate rocks of Saar Formation as well as fractured basement rocks (e.g., King et al. 2003; Hakimi et al. 2012b; Al-Areeq and Alaug 2014; Al-Areeq et al. 2015; Lashin et al. 2016; Khamis et al. 2017).

SAMPLES AND EXPERIMENTAL METHODS

The dataset of this study consists of 12 cutting samples from two wells: Kharir 1-27 and Kharir 3-07, provided by the Total Oil company, Republic of Yemen, in addition to the organic geochemical results of 23 cutting samples selected from two wells: Sunah-1 and Al-Qarn-1, released from the Yemeni authority of petroleum exploration and production (PEPA) (Fig. 1a).

The samples were selected to represent the argillaceous limestone intervals of the Naifa Formation and were analyzed using a variety of geochemical and petrological methods (Fig. 2). The analyses were conducted at specialized international research centers and laboratories including the Organic Petrology/Geochemical Laboratories at the University of Malaya in Malaysia and the Simon Petroleum Technology Limited Laboratories in the UK.

Organic Geochemical Analyses

The rock samples were crushed, their carbonate minerals were removed using concentrated HCl acid LECO, and then the CS125 and Multi EA2000 elemental analysis instruments were used to measure the total organic carbon (TOC) content. The samples were also subjected to pyrolysis analysis using Rock-Eval II and Weatherford source rock analyzer (SRA)-TOC/total petroleum hydrocarbon (TPH) tools. Several parameters were measured such as the free hydrocarbon content (S_1), the generated

Table 1. Bulk geochemical of TOC and pyrolysis (measured and calculated results) of the analyzed Naifa samples in the onshore Masila Basin

Depth (m)	Pyrolysis data						TOC wt%	Kerogen type
	Measured			Calculated				
	S_1	S_2	T_{\max} (°C)	HI	PI	PY		
<i>Al-Qarn-1 well</i>								
2452	0.02	0.80	438	136	0.02	0.82	0.59	III
2460	0.02	0.61	437	115	0.03	0.63	0.53	III
2472	0.03	1.51	440	210	0.02	1.54	0.72	II–III
2476	0.04	1.35	439	201	0.03	1.39	0.67	III
2480	0.03	1.70	441	224	0.02	1.73	0.76	II–III
2484	0.08	1.11	440	206	0.07	1.19	0.54	II–III
2488	0.02	0.91	439	172	0.02	0.93	0.53	III
2526	0.12	1.08	440	212	0.10	1.20	0.51	II–III
2670	0.04	2.69	438	374	0.10	2.73	0.72	II
2706	0.20	1.63	439	223	0.11	1.83	0.73	II–III
2846	0.60	6.74	444	421	0.08	7.34	1.60	II
2850	0.20	2.33	441	306	0.08	2.53	0.76	II–III
2866	0.16	2.41	444	227	0.06	2.57	1.06	II–III
2942	0.06	1.10	444	220	0.05	1.16	0.50	II–III
<i>Sunah-1 well</i>								
2310	0.03	0.58	439	71	0.05	0.61	0.82	III
2400	1.84	6.37	–	245	0.22	8.21	2.60	II–III
2430	0.07	0.99	442	119	0.07	1.06	0.83	III
2457	0.12	1.52	442	150	0.07	1.64	1.01	III
2490	0.30	3.53	434	225	0.08	3.83	1.57	II–III
2510	0.23	3.70	442	224	0.06	3.93	1.65	II–III
2540	0.25	4.67	441	288	0.05	4.92	1.62	II–III
2555	0.36	4.22	435	327	0.08	4.58	1.29	II
2570	0.53	9.66	440	433	0.05	10.19	2.23	II
<i>Kharir 1-27 well</i>								
2370	0.07	1.10	439	114	0.06	1.17	0.97	III
2375	0.05	0.59	439	68	0.07	0.64	0.87	III
2380	0.04	0.95	432	91	0.04	0.99	1.04	III
2390	0.06	1.03	430	85	0.06	1.09	1.21	III
2395	0.01	3.43	439	260	0.01	3.44	1.32	II–III
2400	0.05	0.82	431	95	0.06	0.87	0.86	III
2410	0.09	1.49	432	140	0.06	1.58	1.07	III
2460	0.01	0.40	430	50	0.02	0.41	0.80	III
<i>Kharir 3-07 well</i>								
2500	0.04	5.14	439	289	0.01	5.18	1.78	II–III
2520	0.04	0.74	439	87	0.05	0.78	0.85	III
2540	0.06	0.82	435	88	0.07	0.88	0.94	III
2560	0.20	4.70	436	270	0.04	4.90	1.74	II–III

TOC total organic carbon content (wt%), S_1 volatile hydrocarbon (HC) content (mg HC/g rock), S_2 remaining HC generative potential (mg HC/g rock), HI hydrogen index = $S_2 \times 100/\text{TOC}$ (mg HC/g TOC), PI = production index = $S_1/(S_1 + S_2)$, PY = petroleum potential yield = $S_1 + S_2$, T_{\max} = temperature at maximum generation

amount of hydrocarbons (S_2), and the maximum temperature of the pyrolysis yield (T_{\max}). In addition, some important parameters according to Espitalié et al. (1977) and Peters and Cassa (1994) were calculated, namely hydrogen index (HI = $S_2 \times 100/\text{TOC}$, mg HC/g TOC), production index [PI = $S_1/(S_1 + S_2)$], and petroleum yield (PY = $S_1 + S_2$) (Table 1). Subsequently, 10 analyzed samples

were selected for further investigations (petrographic and geochemical) including bitumen extraction, gas chromatography–mass spectrometry (GC–MS), pyrolysis–GC (Py–GC), visual kerogen, spore coloration, and vitrinite reflectance measurements (VRo).

For bitumen analysis, 10 shale samples were extracted with a mixture of dichloromethane and

methanol (93:7) for 72 h using the Soxhlet instrument. The extracted bitumen was fractionated by employing the liquid column chromatography technique on silica gel topped with alumina oxide and was segregated into saturated, aromatic and polar fractions using petroleum ether (100 ml), dichloromethane (100 ml), and methanol (50 ml), respectively. A full scan mode of 50–550 amu was performed during the GC–MS analysis. The GC experimental analysis operated with HP-5MS5 column with the following dimensions: 30 m long, 0.32 mm of internal diameter and 0.25 μm of film thickness. The temperature range of 40–300 °C was applied at a rate of 4 °C/min. The 300 °C temperature was held on the samples for a 30-min time.

The aliphatic fraction was analyzed using a gas chromatography-mass spectrometry (GC–MS, HP 5975B MSD MS). The GC of the GC–MS was attached to the ion source defined by the following parameters: 70 eV ionization voltage, 100 milliamps filament emission and 230 °C interface temperature (Adegoke et al. 2017). The ion monitoring capabilities of the data acquisition system were selected to allow monitoring of previously published specific ions of the saturated hydrocarbon ratios, such as *n*-alkanes (m/z 85), triterpanes (m/z 191), and steranes (m/z 217) (Peters et al. 2005; Adegoke et al. 2017). To quantify the terpane and sterane distributions, the peak heights were measured in the m/z 191 and m/z 2017 chromatograms, respectively (“Appendix 1”).

Besides the GC–MS experimental examination of the extracted samples, their kerogen composition, type, and structural characteristics were analyzed using a Py–GC instrument (Horsfield 1989; Horsfield and Dueppenbecker 1991). Solvent-extracted rock samples of approximately 1–2 mg were analyzed using an Agilent GC chromatograph HP-Ultra1, 50 m \times 32 mm equipped with a dimethylpolysiloxane-coated column and a film ionization detector. The applied temperature range was released over 300–600 °C at 25 °C/min, and a nitrogen-cooled trap was used to collect the pyrolysis products. The resultant peaks were identified on the basis of reference chromatograms using the manual interface of Agilent ChemStation software and by comparing the values to published data (Dembicki et al. 1983; Abdullah 1999; Harry 2008; Dembicki 2009; Hakimi et al. 2013; Adegoke et al. 2015).

Organic Petrographic Analyses

Organic petrographic examinations were executed on the 10 analyzed samples using polished block and slide techniques. The polished block sample analysis was conducted with oil immersion under plane-polarized reflected light using a LEICA DM 6000 M microscope for vitrinite reflectance measurement. The VRo measurement of each sample is based on a sapphire glass calibration with standard reflectance value 0.589%, and the measured VRo values were reported as the arithmetic means of 10–15 measurements.

The extracted rock samples were subsequently subjected to kerogen isolation using the specifications of Durand and Monin (1980) and Horsfield (1989). Different acids such as hydrofluoric (HF) and hydrochloric (HCl) were utilized for separating the kerogen organic matter from the inorganic rock matrix. Hot HCl was used mainly to remove carbonates, whereas 60% of hot HF was used for silicate breakdown and removal. A combination of zinc bromide flotation and ultrasonic vibration was applied for separation of mineral residues from the kerogen. The residues were then mounted onto glass slides in glycerin jelly and were examined under the aforementioned microscope at different magnifications. Isolated kerogen palynofacies analysis was performed under plane-polarized transmitted white light using a microscope to identify the various organic matter groups such as amorphous (AOM), phytoclasts, and palynomorphs. The calculation of organic matter percentage and their frequency was conducted per sample by counting of 200 organic matter particles following the rules of Nøhr-Hansen (1989).

RESULTS

Organic Matter Richness and Generation Potential

Determination of the TOC content of a source rock provides information on its richness of organic matter and potential volume of hydrocarbon generation during maturation (Peters and Cassa 1994; Hunt 1996). The analyzed Naifa samples have variable values of TOC in the range of 0.50–2.60% (Table 1). The TOC data show that the most of the analyzed samples exhibited relatively low TOC of less than 1% ($n = 20$ samples), followed by samples

with TOC of > 1% ($n = 13$ samples), and only two samples with TOC of > 2% (Table 1). The TOC data clarify that the studied Naifa samples are mainly marginally organic-rich to organic-rich and attain fair to good potential source rocks according to Tissot and Welte (1984), Peters and Cassa (1994), and Hunt (1996). The pyrolysis S_1 and S_2 yields were in the range 0.01–1.84% and 0.40–9.66 mg HC/g rock, respectively (Table 1), and these values together make up the potential PY, which is in the range of 0.41–10.19. The potential PY and the measured TOC indicate that the analyzed Naifa samples are generally fair to good source rocks potential for hydrocarbon generation (Fig. 3a).

The hydrocarbon generation potential of the analyzed samples was also inferred from the bitumen content of the extracted organic matter (EOM). The amount of EOM and its saturated, aromatic hydrocarbons, and nitrogen, sulfur, or oxygen (NSO) proportions are listed in Table 2. The detected range of the EOM values, 511.28–1278.24 ppm (Table 2), indicates consistency with the measured values of TOC and was classified as fair to good potential source rocks (Fig. 3b).

In addition, the EOM of the analyzed samples has high amounts of NSO components in the range of 52.16–70.97% (Table 2). In contrast, the saturated and aromatic hydrocarbons are represented in lower fractions at ranges of 11.29–32.73% and 13.60–33.33%, respectively (Table 2). However, the Naifa samples with the highest yields of NSO components were identified within a depth interval of 2370–2560 m, which can be attributed to the early-mature source rocks as previously reported by Peters et al. (2005). The high NSO contents in the analyzed Naifa samples also suggest that they contain greater amounts of plant-derived organic matter, as indicated by the kerogen type based on the pyrolysis and petrological analyses (Tables 1 and 3).

Bulk and Quantitative Kerogen Type

The bulk characterization of the kerogen type was assessed based on the calculated Rock–Eval HI data (Table 1). Most of the analyzed samples have HI values of 50–306 mg HC/g TOC and indicate mainly Type III and III/II kerogens except for four samples with HI values of more than 320 mg HC/g TOC. Thus, the type is II kerogen (Peters and Cassa 1994). The bulk kerogen type was further analyzed by using

a modified Van Krevelen diagram of HI vs. T_{\max} (Fig. 4). Types III and II/III were the dominant kerogen in the analyzed Naifa samples, with minor contribution of Type II. In addition, the T_{\max} values of the analyzed Naifa samples were in the range of 430–444 °C. This result indicates that the analyzed Naifa samples contain early-mature organic matter in which the thermal alteration level was not strong enough to generate commercial petroleum (Espitalié 1985).

The kerogen type illustrated from bulk pyrolysis performed in this study matches reasonably with the results derived from the open Py–GC. This offers a very powerful quantitative method for detecting the composition of the kerogen decomposed thermally during its maturity using the pyrolysis products (Fig. 5a). The pyrolysis products of the analyzed samples contain *n*-alkene/alkane homologous series with important aromatic hydrocarbon components such as benzene, toluene, and *m*-*p*-xylene as shown in the pyrograms of Figure 5a. In addition to these components, phenolic compounds were also recognized in the analyzed samples (Fig. 5a). The sources of aromatic and phenolic compounds were derived from vitrinite of high plant materials (Muscio and Horsfield 1996). Note that the pyrolysate characteristics indicate high contribution of terrigenous organic assemblages in the analyzed Naifa samples (e.g., Horsfield 1997; Hakimi et al. 2013; Togunwa et al. 2015). The distribution of the *m*-*p*-xylene, phenol, and *n*-octene pyrolysate compounds and their percentages enabled further assessment of the organo-facies in the analyzed samples using a slightly modified ternary diagram of Larter (1984) and Abdullah et al. (2017). Accordingly, the kerogen was characterized as predominant of Type III and mixed Type II/III (Fig. 5b).

Visual Kerogen

Principal visual analysis was conducted on the kerogens isolated from the 10 extracted samples and was used to investigate the main palynofacies; the results are presented in Table 3. The main identified palynofacies were mostly structured organic matter including phytoclasts and palynomorphs in addition to structureless and amorphous organic matter (AOM). The palynofacies are characterized by a dominance of phytoclasts such as woody tissue and cuticles (Fig. 6) and the presence of significant quantities of sporomorphs, which are mainly spores

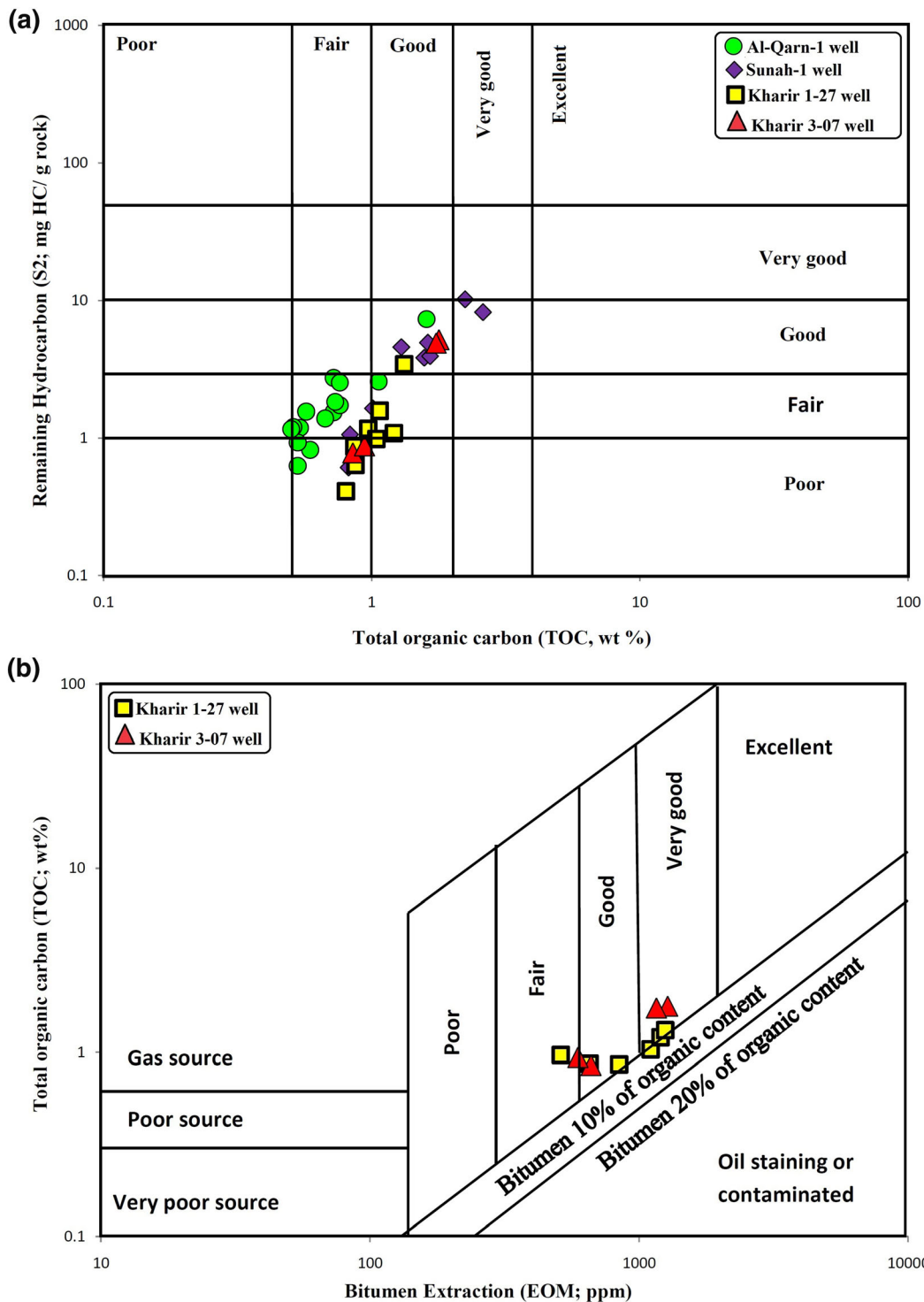


Figure 3. Cross-plots, for the analyzed Naifa samples, of TOC vs. PY of (a) petroleum and (b) extractable bitumen.

Table 2. Relative proportions of saturated, aromatic hydrocarbon fractions, and NSO compounds and ratios based on *n*-alkanes and isoprenoids distributions of the analyzed bitumen fraction of the Naifa samples

Depth (m)	Bitumen extraction and chromatographic fractions (% of whole rocks)					<i>n</i> -alkanes and acyclic isoprenoids				
	EOM (ppm)	Sat. (%)	Aro. (%)	NSO (%)	HC (%)	Pr/Ph	Pr/ <i>n</i> -C ₁₇	Pr/ <i>n</i> -C ₁₈	CPI	WI
<i>Kharir 1-27 well</i>										
2370	511.28	11.29	17.74	70.97	29.03	1.35	0.70	0.49	1.07	1.50
2375	653.66	23.08	22.56	54.36	45.64	1.61	0.57	0.29	1.16	1.31
2380	1102.72	25.88	13.60	60.53	39.48	1.38	0.70	0.48	1.07	1.50
2390	1200.13	31.03	16.81	52.16	47.84	1.30	0.65	0.47	1.20	1.14
2395	1249.78	19.51	13.98	66.51	33.49	1.26	0.73	0.56	1.18	1.13
2410	841.62	32.73	14.09	53.18	46.82	1.28	0.61	0.48	1.20	1.20
<i>Kharir 3-07 well</i>										
2500	1278.24	15.07	24.66	60.27	39.73	1.35	0.54	0.30	1.22	1.17
2520	663.43	13.45	33.33	53.22	46.78	1.31	0.61	0.42	1.20	1.25
2540	592.30	18.18	29.29	52.53	47.47	1.35	0.66	0.46	1.16	1.62
2560	1160.66	17.14	18.37	64.49	35.51	1.67	0.72	0.40	1.24	1.56

EOM bitumen extraction (ppm), *Sat.* saturation fractions, *Aro.* aromatic fractions, *HC* hydrocarbon fractions = (saturation + aromatic) CPI = carbon preference index: $\{2(C_{23} + C_{25} + C_{27} + C_{29}) / (C_{22} + 2[C_{24} + C_{26} + C_{28}] + C_{30})\}$
 WI = waxiness index = $\sum(n-C_{21}-n-C_{31}) / \sum(n-C_{15}-n-C_{20})$

Table 3. Palynofacies (%) and thermal maturity indicators (vitrinite reflectance measurements (VRo) and thermal alteration index (TAI) and pyrolysis GC) of the extracted Naifa samples

Depth (m)	Maturity		Palynofacies (%)				Pyrolysis GC (%)			Kerogen typing
	VRo (%)	TAI	Phytoclasts	Amorphous (AOM)	Palynomorphs		m(+p)-xy-lene	<i>n</i> -C8 <i>n</i> -octene	Phenol	
					Spore + Pollen	Marine microfossils				
<i>Kharir 1-27 well</i>										
2370	0.65	2	110	57	33	3	27	33	40	III
2375	0.64	2	84	80	60	3	30	15	55	III
2380	0.69	2	78	60	50	5	50	13	37	III
2390	0.65	2	78	60	48	4	36	15	49	III
2395	0.66	2	75	60	44	8	25	38	37	II-III
2410	0.68	3	78	53	33	5	32	14	54	III
<i>Kharir 3-07 well</i>										
2500	0.70	3	75	59	53	10	55	29	16	II-III
2520	0.68	3	73	46	47	7	33	14	53	III
2540	0.68	3	80	69	48	7	40	17	43	III
2560	0.65	2	85	45	25	13	33	31	36	II-III

(Fig. 7). Minor dinoflagellate cysts were also recognized in the analyzed samples (Fig. 7), which indicate a marine environment during deposition of the Naifa sediments with lower than normal salinity conditions (Batten and Stead 2005). This palynofacies composition also implies high proportions of Type III and II/III kerogen, as addressed from the ternary diagram of AOM, phytoclasts, and palynomorph (Fig. 8). This is consistent with geochemical pyrolysis data in terms of bulk and quantitative results, as discussed in the preceding section.

n-Alkanes, Acyclic Isoprenoids, and Waxiness

The distribution of identified *n*-alkanes and acyclic isoprenoids was based on *m/z* 85 mass chromatograms (Fig. 9). The normal alkane and acyclic isoprenoid hydrocarbons generally show unimodal-dominated *n*-alkanes and isoprenoids distribution and the carbon number ranges from short-to medium-chain *n*-alkane (*n*-C₁₂-*n*-C₂₀) to molecular weight compounds with long-chain *n*-alkane (+*n*-C₂₅) (Fig. 9). A predominance of *n*-alkane distribu-

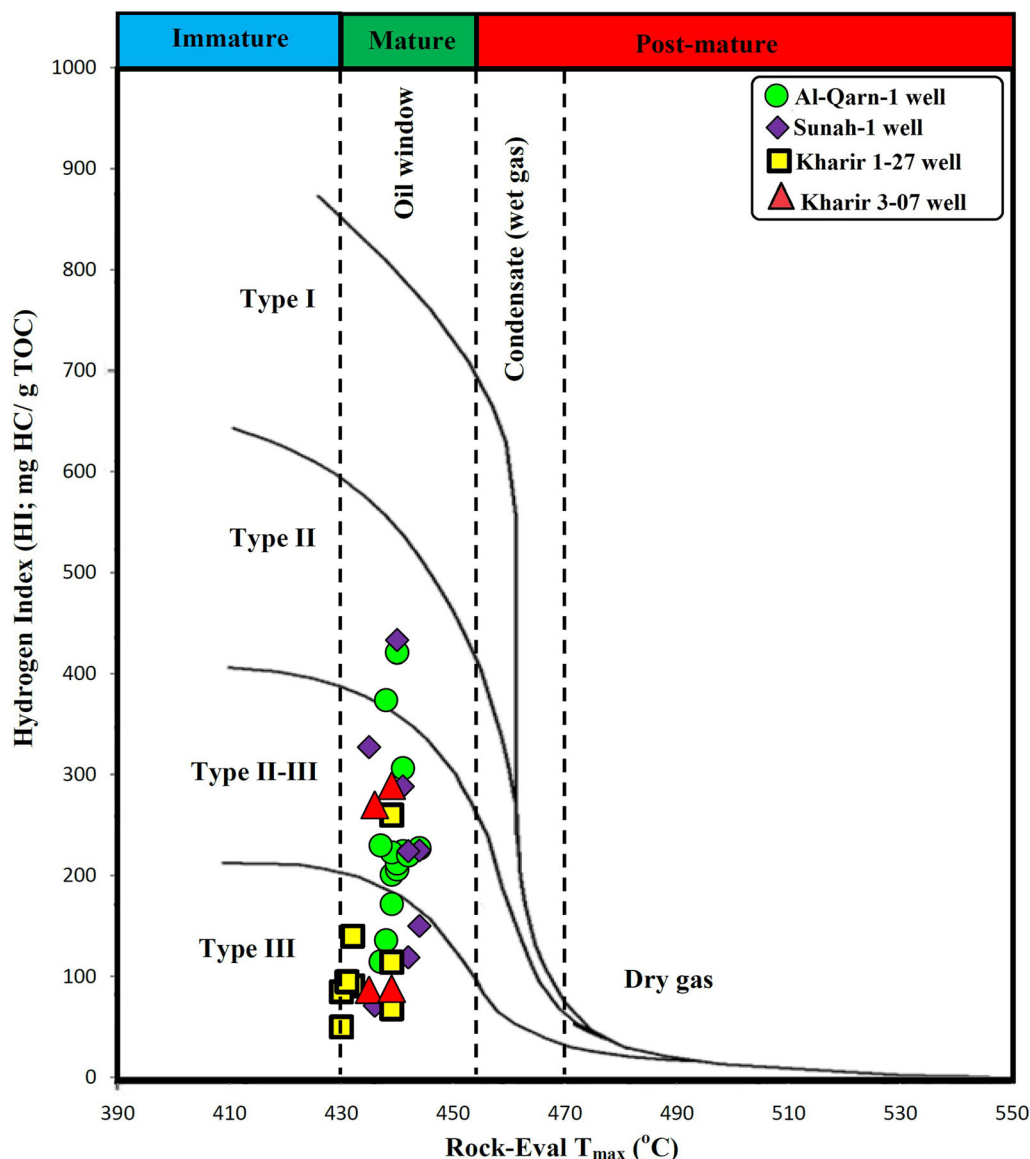


Figure 4. Characteristics of kerogen in the analyzed Naifa samples based on Rock–Eval HI vs. T_{\max} .

tions in the C_{23} – C_{29} region was recognized for all samples (Fig. 9). Hence, their carbon preference index (CPI) and waxiness (WI) values are high, at 1.07–1.24 and 1.13–1.62, respectively (Table 2). Pristane and phytaneacyclic isoprenoids are present in significant amounts in all of the analyzed samples (Fig. 9). Pristane is generally abundant in all samples, and the pristane/phytane (Pr/Ph) ratios are low with values in the range of 1.26–1.67 (Table 2). Furthermore, the amounts of isoprenoid compared to n -alkanes (Fig. 8) in terms of pristane/ n - C_{17} and phytane/ n - C_{18} ratios were also calculated and re-

corded relatively low values of 0.44–0.73 and 0.29–0.49, respectively (Table 2).

Terpanes, Steranes, and Diasteranes

The ion m/z 191 and m/z 217 of the GC–MS mass fragmentograms show the presence of terpanes, steranes, and diasteranes in the analyzed Naifa samples (Fig. 10). The m/z 191 mass fragmentograms of the extracted samples display high hopanes relative to tricyclic terpanes in all of the

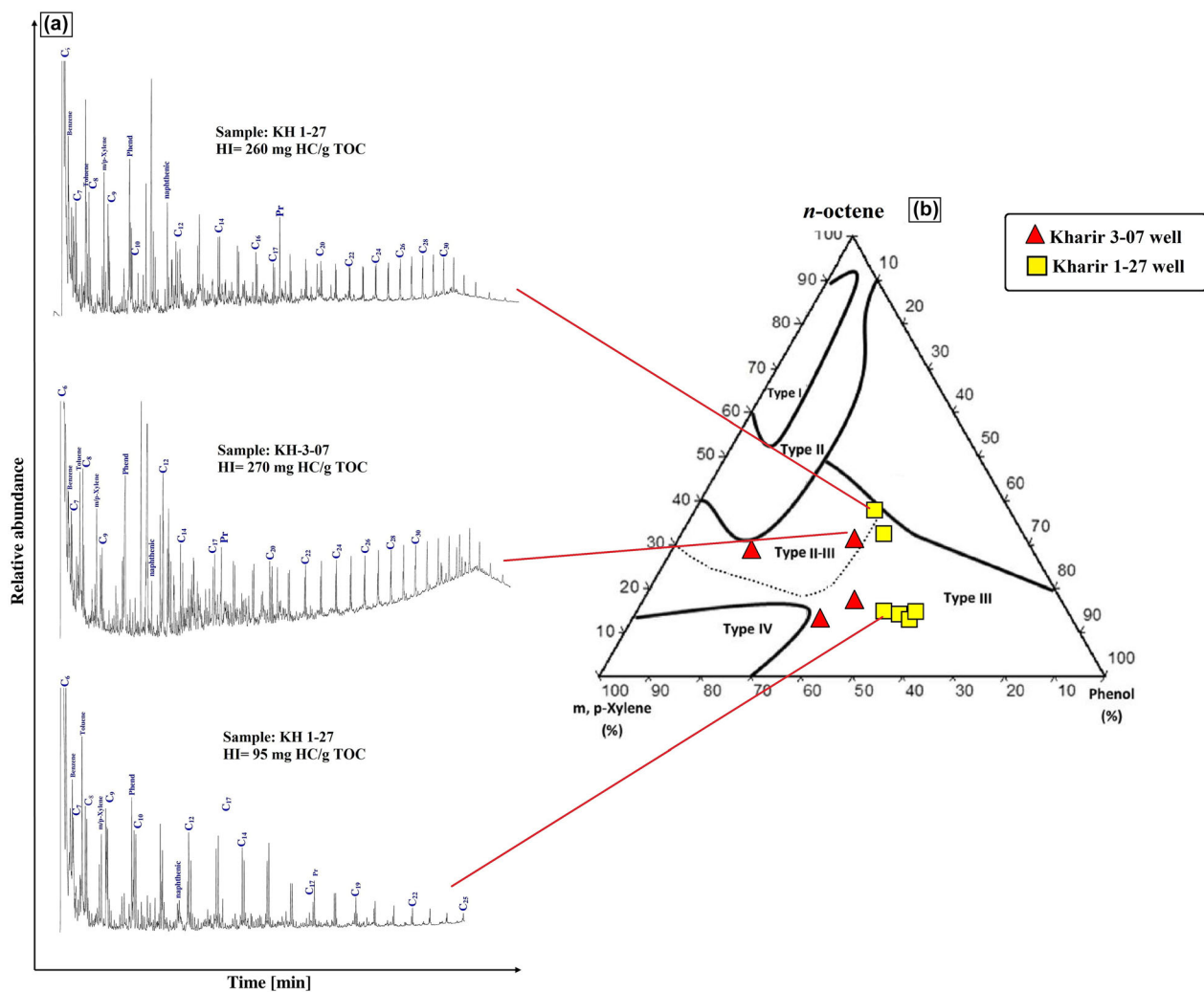


Figure 5. Quantitative pyrolysis (Py-GC) of selected extracted samples from two wells in the Naifa Formation, Kharir 1-27 and Kharir 3-07, showing (a) the pyrolysate distribution of *n*-alkene/alkane doublets and aromatic with phenolic compounds and (b) the characteristics of kerogen based on the relative percentage of three pyrolysate compounds, *m*-*p*-xylene, phenol, and *n*-octene, plotted on the ternary diagram of Larter (1984) and Abdullah et al. (2017).

analyzed samples (Fig. 10a). The biomarker analysis reveals that C_{30} -hopane and C_{29} -norhopane are also dominant. However, according to the C_{29}/C_{30} ratios of generally more than 0.80, the content of C_{29} -norhopane is mostly slightly higher than that of C_{30} 17α (H) hopane (Fig. 10a, Table 4), which suggests carbonate-rich facies in most of the analyzed samples (Waples and Machihara 1991).

In all of the analyzed samples, the homohopanes are characterized by high abundances of C_{31} series and generally decreases toward the C_{35} (Fig. 10a). The C_{31} -22R-hopane/ C_{30} -hopane ratios for the analyzed samples range from 0.32 to 0.43

(Table 4). Besides, significant (18-(H)-22,29,30-trisnorneohopane) (Tm) and considerable quantity of 18α -(H)-22,29,30-trisnorneohopane (Ts) are also present (Fig. 10a), with higher Tm/Ts values in the range of 2.5–11.3 (Table 4). In addition, both C_{32} $\alpha\beta$ -homohopane isomerization ($22S/(22S + 22R)$) and C_{30} -moretane/ C_{30} -hopane ratios were calculated to be 0.54–0.57 and 0.31–0.54, respectively (Table 4).

Figure 10B shows the sterane and diasterane distributions in three representative analyzed samples. The C_{27} and C_{29} steranes are predominant over the C_{28} homologues, with relative proportions

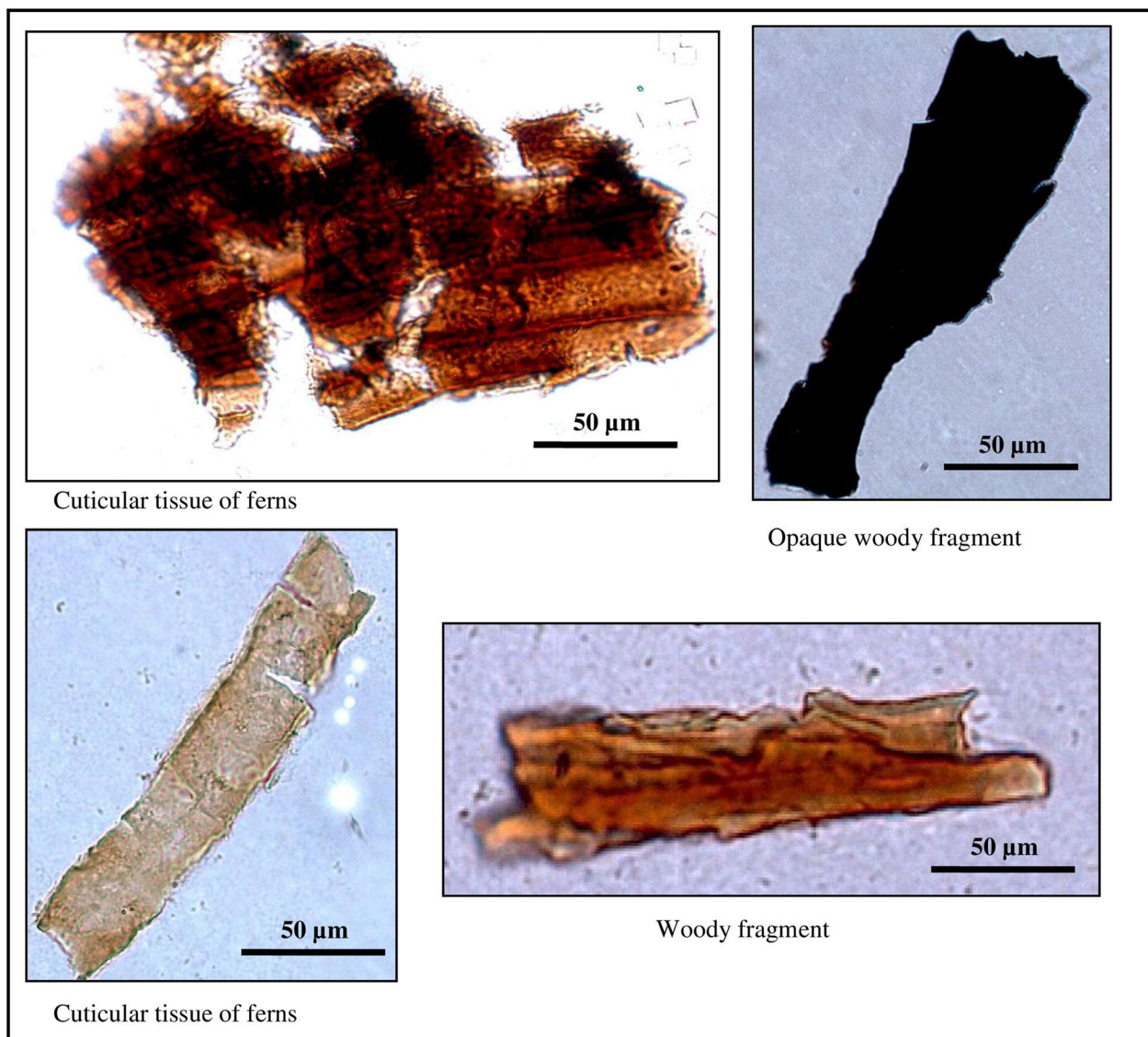


Figure 6. Phytoclasts of mainly cuticle and plant fragments of plant secretion from the analyzed Naifa samples from two wells, Kharir 1-27 and Kharir 3-07, as listed in Table 3.

of 42.9–48.7%, 35.1–40.9%, and 15.2–18.6%, respectively (Table 4). These proportions can be clearly demonstrated by the relatively low C_{29}/C_{27} regular sterane ratios of less than unity (Table 4). The ratios of diasterane/sterane are low in all of the analyzed samples (Table 2) and provide support for a carbonate-rich facies as previously reported (e.g., Mohialdeen and Hakimi 2016). Additionally, maturity biomarker ratios such as $20S/(20S + 20R)$ and $\alpha\beta\beta/(\alpha\beta\beta + \alpha\alpha\alpha)$ for C_{29} -sterane were calculated (Table 4).

DISCUSSION

Organic Matter Input

The short- to medium ($n-C_{14}$ – $n-C_{20}$)-chain n -alkane distributions, with a significant long-chain n -alkane ($+n-C_{25}$) molecular weight compounds (Fig. 9), appear to indicate that the Naifa sediments contain mixed organic matter with significant terrigenous organic matter input (Colombo et al. 1989; Peters et al. 2005).

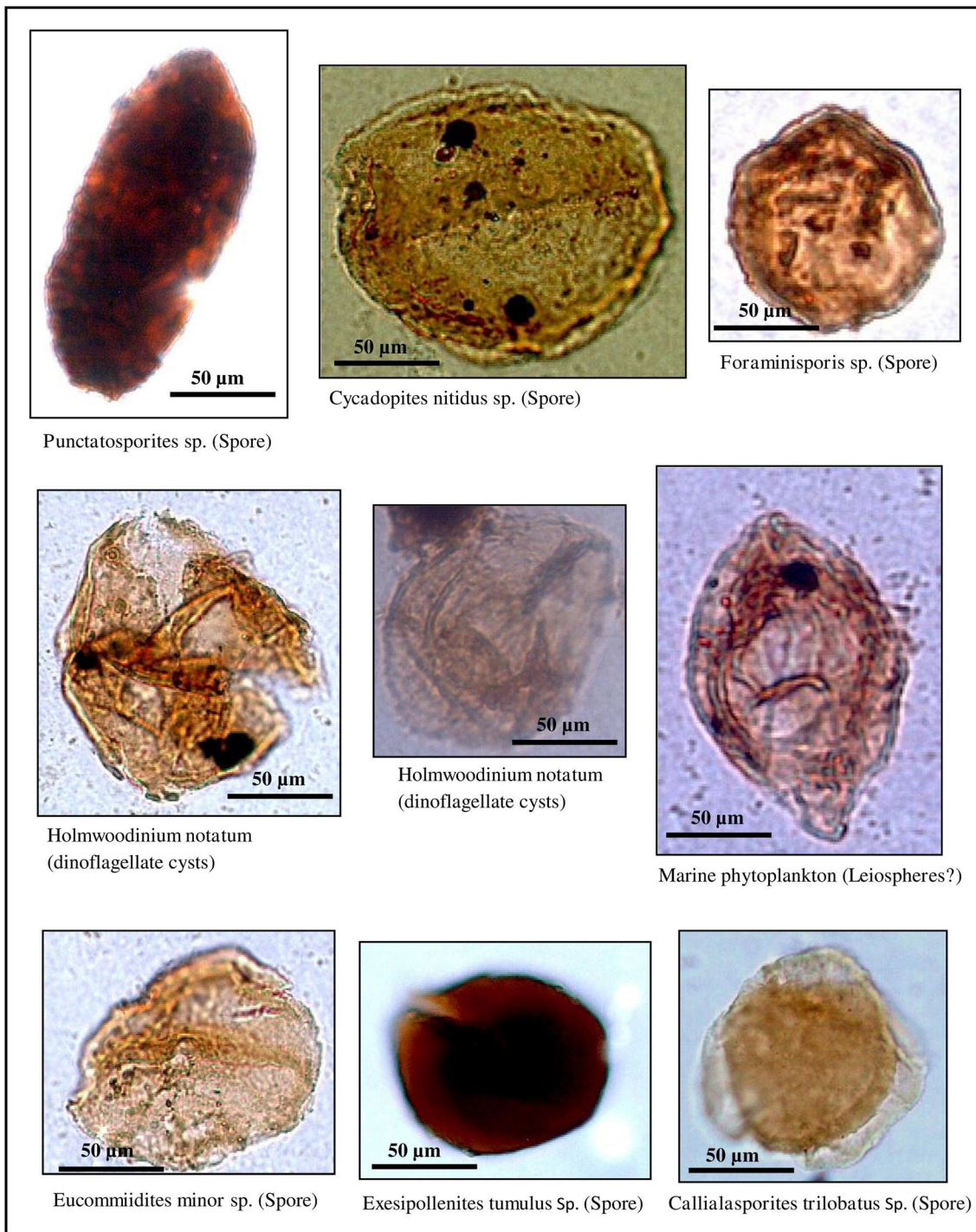
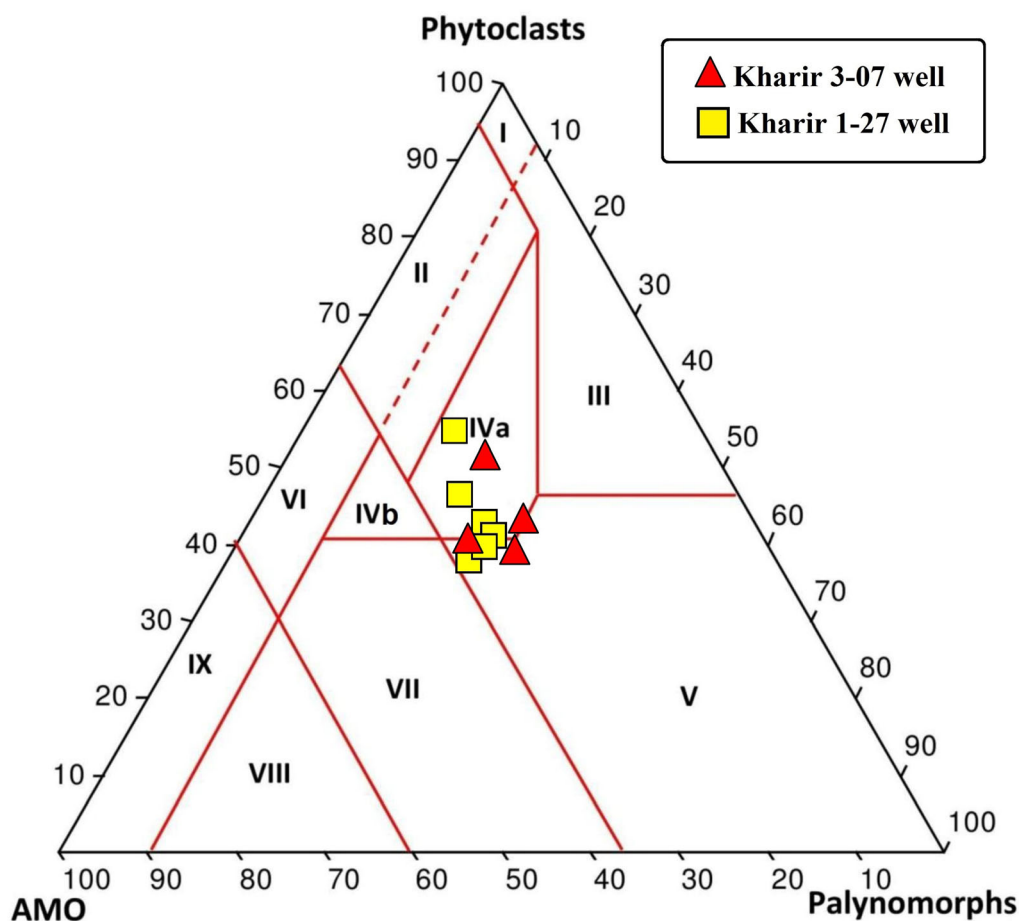


Figure 7. Structured organic matter of the dinoflagellate cyst species, marine phytoplankton, and spores macerated from the analyzed Naifa samples from two wells, Kharir 1-27 and Kharir 3-07.



Palynofacies field	Environment	Kerogen type
I	Highly proximal shelf or basin.	III (gas prone)
II	Marginal dysoxic-anoxic basin.	III (gas prone)
III	Heterolithic oxic shelf ("proximal shelf").	III or IV (gas prone)
IV	Shelf to basin transition.	III or II (mainly gas prone)
V	Mud- dominated oxic shelf ("distal shelf").	III > IV (gas prone)
VI	Proximal suboxic-anoxic shelf.	II (oil prone)
VII	Distal dysoxic-anoxic "shelf".	II (oil prone)
VIII	Distal dysoxic-anoxic shelf.	II >> I (oil prone)
IX	Distal suboxic-anoxic basin.	II ≥ I (highly oil prone)

Figure 8. Ternary diagram of amorphous organic matter–phytoclcasts–palynomorph (APP) kerogen plot used to characterize the kerogen assemblage and environments under transmitted light microscopy (modified after Tyson 1995).

The ratios of isoprenoids (pristane/phytane) vs. normal alkanes (phytane/ n -C₁₇) reflect an organic matter accumulation of mixed marine–terrestrial

sources (Fig. 11a). In addition, the relatively high CPI values with odd over even predominance in the analyzed samples indicate an early thermal maturity

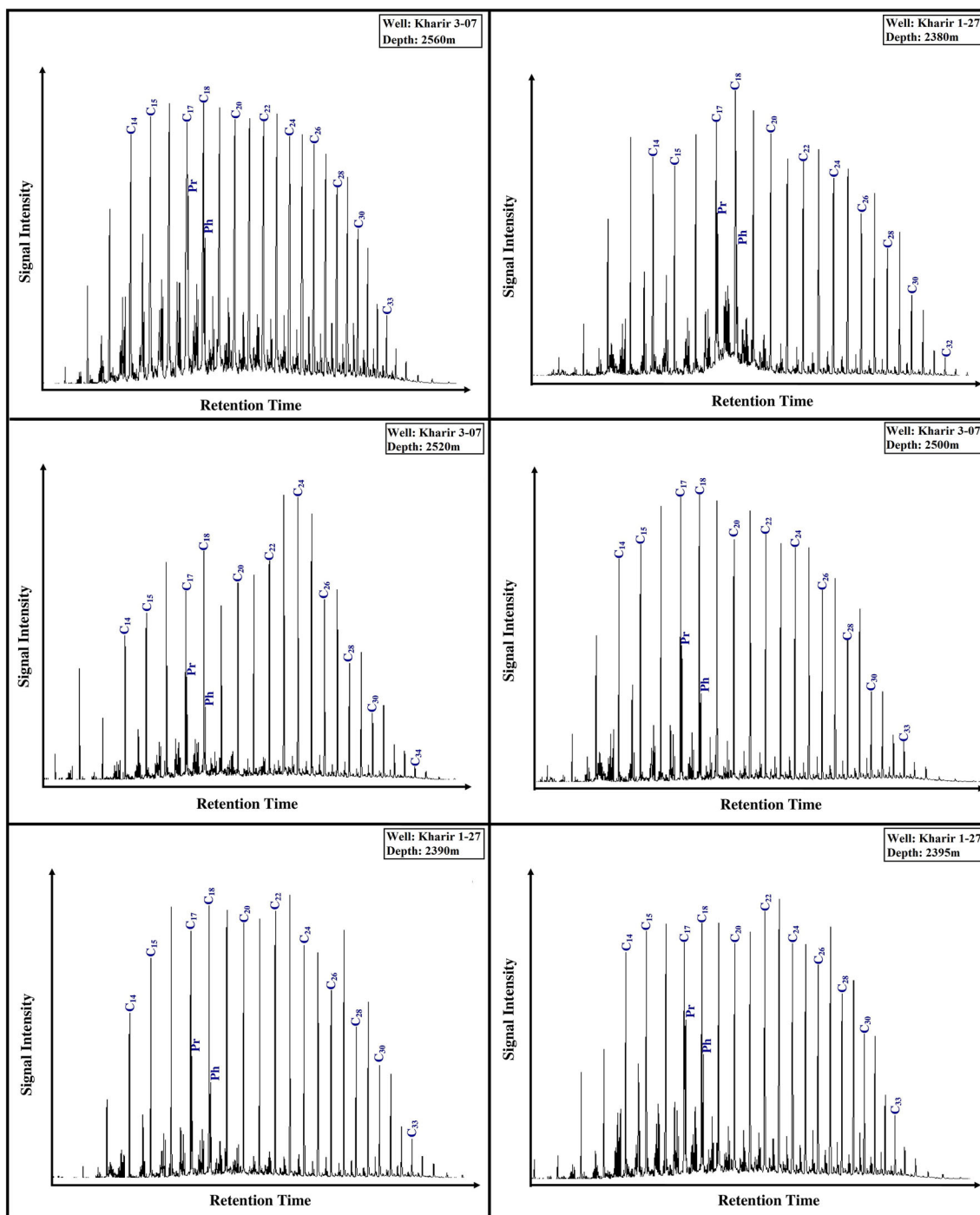


Figure 9. Mass fragmentograms of m/z 85 of saturated hydrocarbons for six analyzed representative Naifa samples.

of the Naifa sediments and indication of a high contribution of terrigenous source input (Fig. 11b). The strong inference of the land plant input in the

analyzed Naifa samples is supported by the high Tm/Ts ratios (Table 4; Fig. 10a). The high relative abundance of Tm compared to Ts has been reported

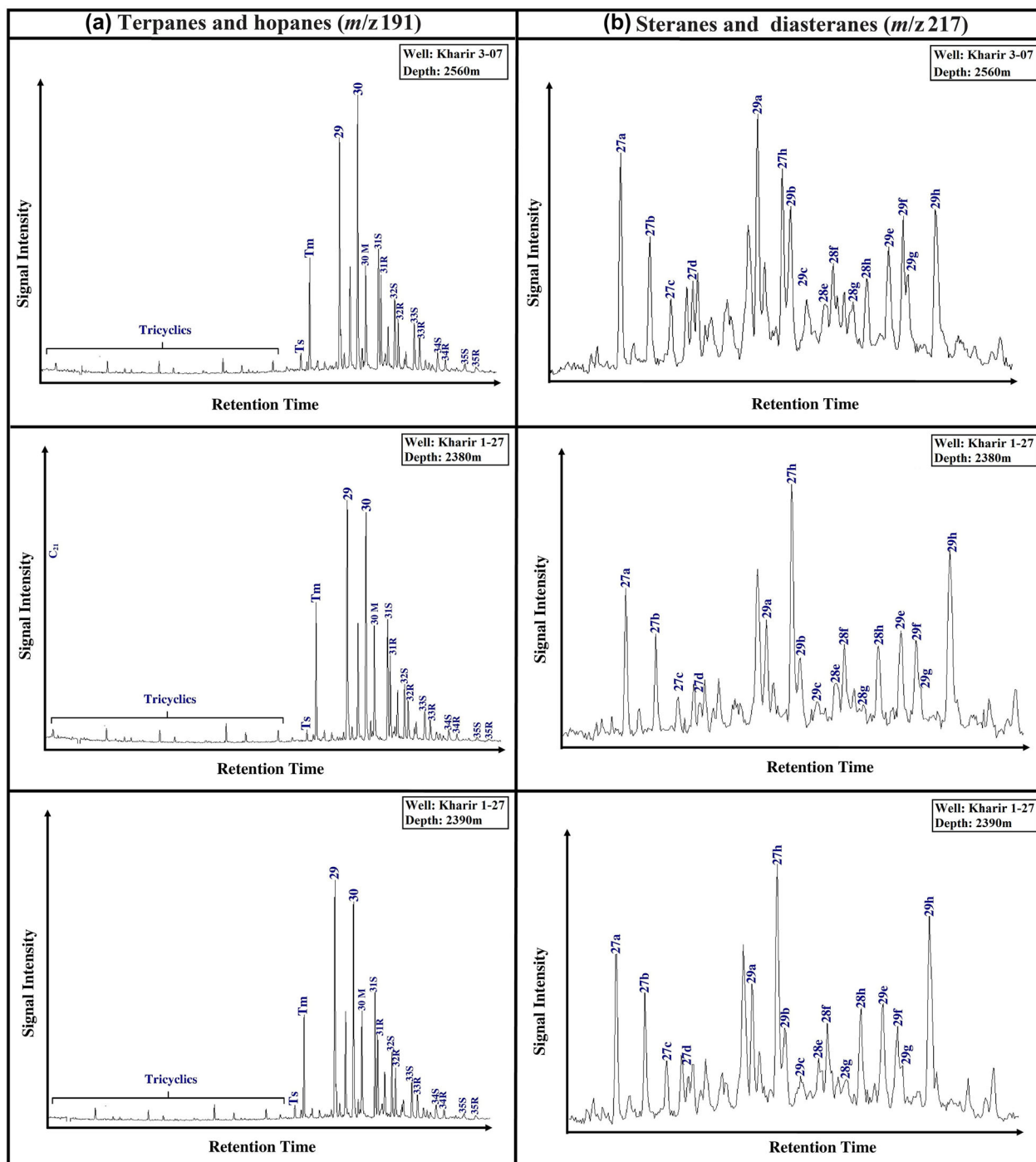


Figure 10. m/z 191 mass fragmentograms (left) and m/z 217 mass fragmentograms (right) of saturated hydrocarbon fractions of three analyzed representative Naifa samples.

to be associated with terrestrially derived organic matter as well as carbonate facies (e.g., Moldowan et al. 1986; Robinson 1987).

The mixed organic matter input in the analyzed samples is also reflected in the distributions of the regular steranes (C_{27} – C_{29}) in the m/z 217 chro-

Table 4. Biomarker ratios of the analyzed Naifa samples illustrating source organic matter input and depositional environment conditions as well as maturity

Depth (m)	Triterpanes and terpanes (<i>m/z</i> 191)				Steranes and diasteranes (<i>m/z</i> 217)							Sterane/hopane
	$C_{32} 22S / (22S + 22R)$	C_{29} / C_{30}	C_{31R} / C_{30H}	Tm/Ts	MC ₃₀ /HC ₃₀	$C_{29} 20S / (20S + 20R)$	$C_{29} \beta\beta / (\beta\beta + \alpha\alpha)$	Regular steranes (%)		$C_{27} / (C_{27} + C_{29})$	Diasterane/sterane	
		C_{30}						C_{27}	C_{28}	C_{29}		
<i>Kharir 1-27 well</i>												
2370	0.54	0.93	0.38	7.0	0.49	0.29	0.29	45.5	15.2	39.3	0.57	0.40
2375	0.55	1.18	0.37	8.4	0.50	0.37	0.37	44.5	18.2	37.3	0.54	0.80
2380	0.56	1.35	0.37	8.6	0.54	0.33	0.33	46.3	16.9	36.8	0.56	0.41
2390	0.54	1.26	0.33	11.3	0.48	0.32	0.29	43.1	17.2	39.7	0.59	0.49
2395	0.55	1.30	0.43	10.8	0.51	0.35	0.37	44.5	18.6	36.9	0.57	0.45
2410	0.56	0.81	0.33	2.5	0.31	0.34	0.38	47.0	15.9	37.1	0.58	0.73
<i>Kharir 3-07 well</i>												
2500	0.56	1.05	0.37	9.8	0.49	0.34	0.33	43.1	17.6	39.3	0.55	0.36
2520	0.57	0.84	0.33	7.2	0.34	0.34	0.29	43.4	16.1	40.5	0.58	0.44
2540	0.55	1.10	0.38	8.4	0.45	0.36	0.33	48.7	16.2	35.1	0.58	0.39
2560	0.56	0.85	0.32	4.3	0.38	0.30	0.29	42.9	16.2	40.9	0.55	0.39

C_{29}/C_{30} = C_{29} -norhopane/ C_{30} -hopane
 C_{31R}/C_{30} = C_{31} regular homohopane/ C_{30} -hopane
 Ts = ($C_{27} 18a$ (H)-22, 29, 30-trisnorhopane)
 Tm = ($C_{27} 17a$ (H)-22, 29, 30-trisnorhopane)
 $C_{30}M/C_{30}H$ = C_{30} -moretane/ C_{30} -hopane

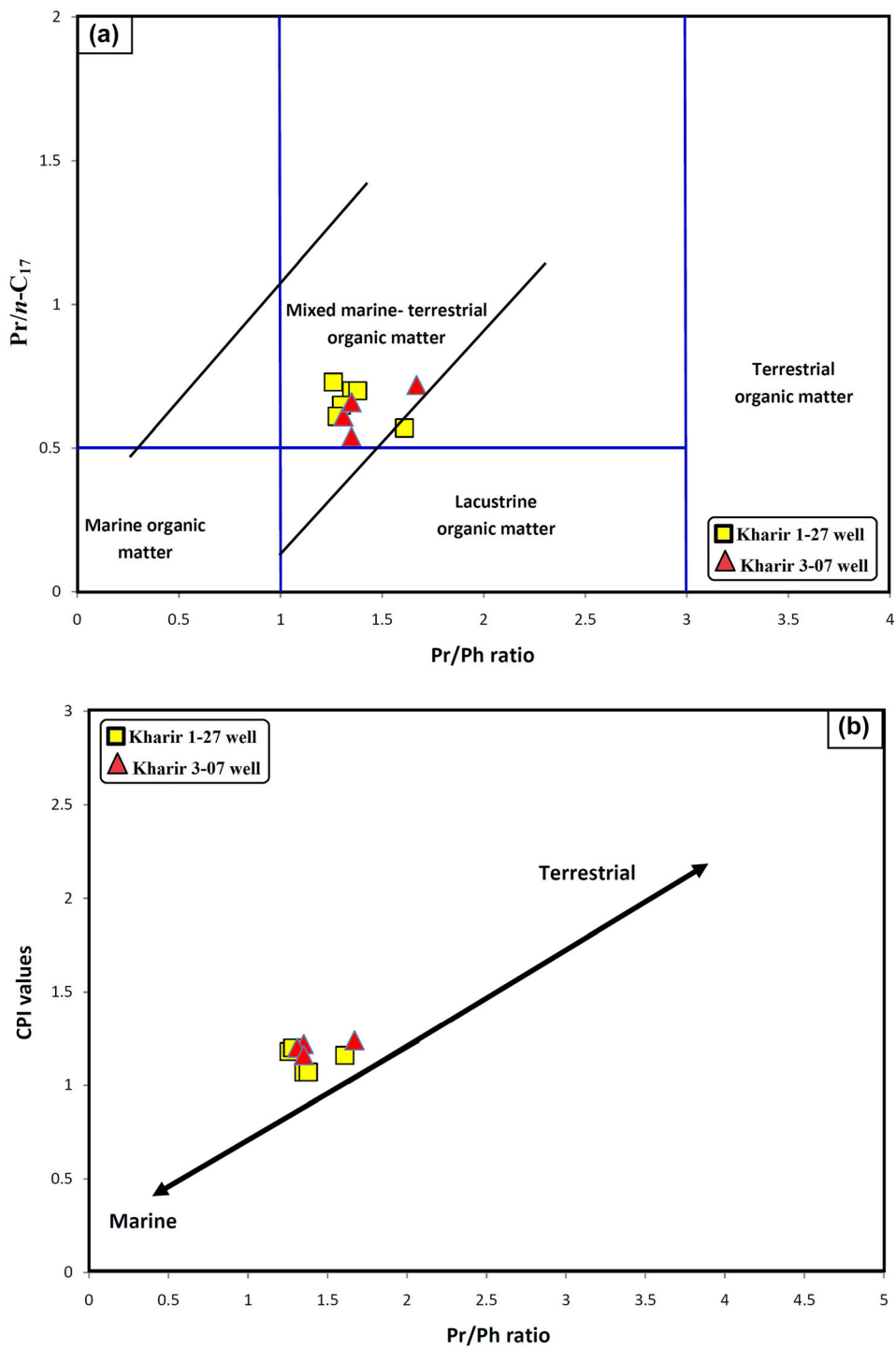


Figure 11. Biomarker cross-plots, for the analyzed Naifa samples, of pristane/phytane vs. (a) pristane/*n*-C₁₇(Pr/*n*-C₁₇) and (b) CPIs.

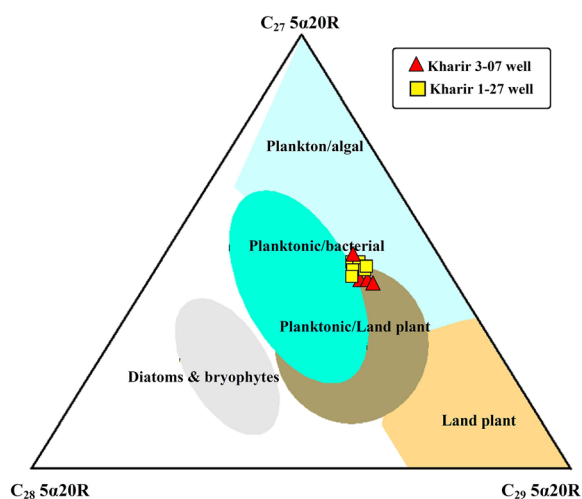


Figure 12. Ternary diagram of regular steranes (C_{27} – C_{29}), indicating the relationship between sterane compositions and the related organic matter input (modified after Huang and Meinschein 1979).

matograms and as reported by previous workers (e.g., Huang and Meinschein 1979; Peters and Moldowan 1993; Peters et al. 2005). These are based on high C_{29}/C_{27} regular sterane ratios and clearly displayed in a ternary diagram of C_{27} – C_{29} $\alpha\alpha\alpha$ -20R steranes (Fig. 12), whereby regular steranes of C_{27} and C_{29} predominate over the C_{28} -sterane in most of the analyzed samples (Fig. 10b; Table 4), indicating mixed organic matter of aquatic planktonic-bacterial and land plant. The notion of mixed source of organic matter with significant contribution from land plants is supported by the geochemical results including Py-GC analysis (Fig. 5) and pyrolysis HI data (Table 1). The latter data relate to the interpretation of kerogen type, which includes mainly Types III and II/III with minor Type II (Fig. 4). This finding of the organic matter is consistent as well with the performed palynofacies analysis (Table 3; Figs. 6 and 7).

Sedimentary Environmental Conditions

In this study, biomarkers were used as broad indicators of sedimentary environment conditions during deposition. The biomarker ratios of C_{31} -22R-homohopane were compared to that of C_{30} -hopane and were used to corroborate that the analyzed Naifa samples in the Say'un–Masila Basin were deposited in an aqueous condition dominated by marine environment as indicated by their high values of more than 0.25 in all of the analyzed samples (Table 4; Peters

et al. 2005). Furthermore, the relationship between C_{31} -22R-hopane/ C_{30} -hopane of the analyzed samples and the Pr/Ph ratios, documented in Figure 13a (modified after Peters et al. 2005), similarly indicates a marine environment. The dinoflagellate cysts recognized in the analyzed samples (Fig. 7) might also be an indication of a marine environment of deposition that prevailed within lower salinity regimes (Batten and Stead 2005).

The C_{29} -norhopane is relatively high in all samples (Fig. 10a), and the C_{29} -norhopane/ C_{30} -hopane ratios range from 0.84 to 1.35, with values mostly > 1.0 (Table 4). This observation suggests that the analyzed samples are likely carbonate-rich rocks such as marls and carbonates that were deposited in a marine environment (Fig. 13b). However, high C_{29}/C_{30} -hopane ratios have been reported in terrestrially derived sediments, especially coal (e.g., Ramanampisoa et al. 1990; Sarki Yandoka et al. 2015a).

The Pr/Ph ratio is a broad indicator commonly used for paleo-redox conditions during deposition (i.e., oxic vs. anoxic) as well as for post-depositional diagenetic alterations (Didyk et al. 1978; Chandra et al. 1994; Escobar et al. 2011). Generally, low Pr/Ph ratios of < 1 suggest anoxic conditions, whereas values between 1 and 3 indicate sub-oxic conditions (Didyk et al. 1978; Chandra et al. 1994; Escobar et al. 2011; Makeen et al. 2015). Comparatively higher values of this ratio, namely > 3, suggest more oxic conditions (Farhaduzzaman et al. 2012; Alias et al. 2012; Sarki Yandoka et al. 2015b).

The analyzed Naifa sediments were likely deposited under sub-oxic conditions with relatively low Pr/Ph ratios between 1.26 and 1.67 (Table 2). This is consistent with the higher organic matter content, as exemplified by relatively high values TOC of > 1% (Table 1). The inference of the sub-oxic condition is supported by geochemical results including the distribution of isoprenoids (pristane/ n - C_{17}) vs. normal alkanes (phytane/ n - C_{18}) in a binary plot (Fig. 14). The palynofacies of isolated kerogen in the analyzed samples also suggest that the Naifa sediments were deposited in a marginally marine environment with strong influx of terrestrial deposits, most likely under sub-oxic environment regimes (Fig. 8).

Thermal Maturity

Knowing the maturity level of the organic matter in the sedimentary rocks is an important parameter for hydrocarbon exploration. The matu-

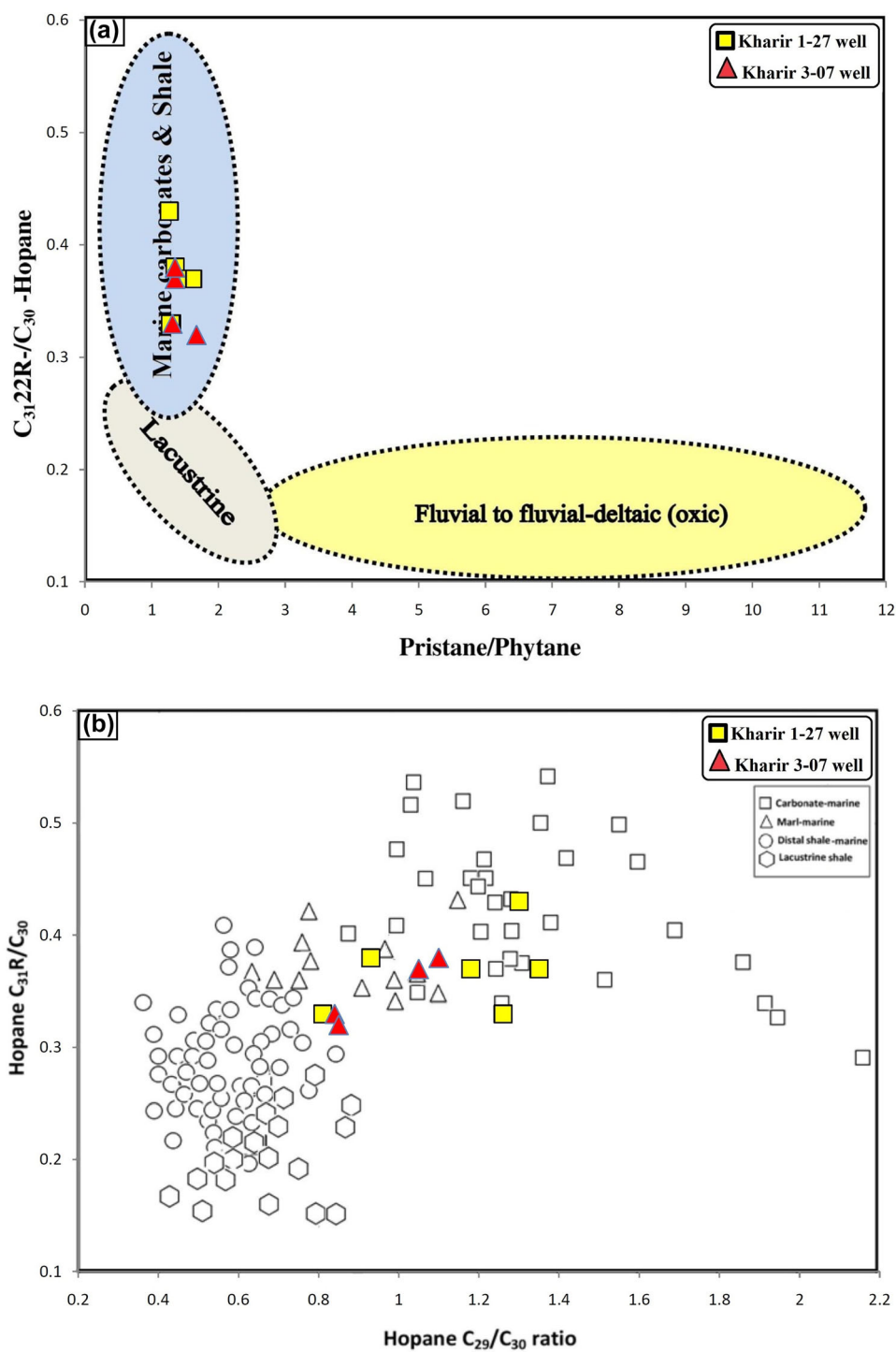


Figure 13. Biomarker cross-plots, for the analyzed samples, of C_{31-22R} -hopane/ C_{30} -hopane ratios vs. (a) pristane/phytane and (b) C_{29} -norhopane/ C_{30} -hopane ratios.

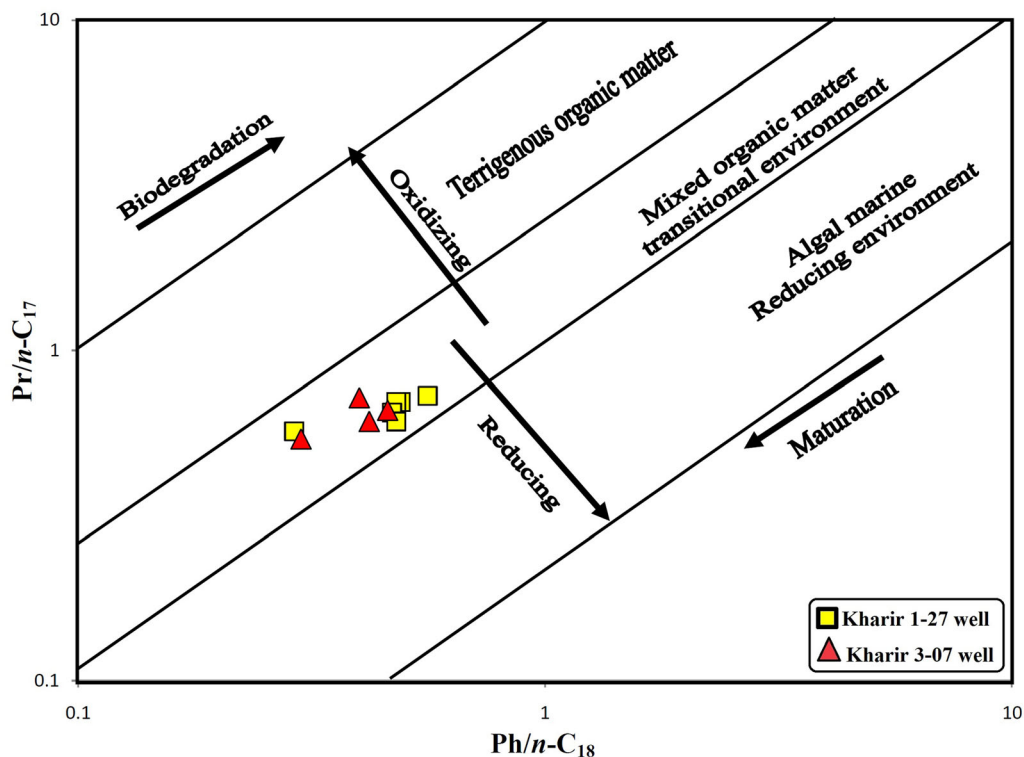


Figure 14. Phytane to n -C₁₈ alkane (Ph/ n -C₁₈) vs. pristane to n -C₁₇ alkane (Pr/ n -C₁₇).

rity of the analyzed Naifa samples was evaluated primarily by using optical methods, i.e., measured VRo and thermal alteration index (TAI) (Table 3). The VRo of organic matter is commonly used to infer the level of maturity in sedimentary rocks (Teichmuller 1958; Manning 1991; Huang et al. 2017). The following maturation stages were recognized at the low end of the oil-window maturity: immature: VRo less than 0.50%, early mature; VRo between 0.50 and 0.70%, peak oil window; VRo is equivalent to 0.70–1.0% and through to 1.3% VRo equivalent to end of the oil-window maturity (Tissot and Welte 1984; Sweeney and Burnham 1990). The VRo of the 10 analyzed Naifa samples ranged from 0.64 to 0.70 (Table 3), indicating oil-window mature equivalent to an early-mature level. This thermal maturity level was confirmed by using other optical method, i.e., TAI that depends mainly on the intensity of spore coloration as a function of maturity (Staplin 1982). The range of the TAI values of the 10 analyzed samples was between 2 and 3 (Table 3), which is consistent with the brown to dark brown color of the spores (Fig. 7) and indicating an

early-mature stage of oil-generation window (Staplin 1982).

In concordance with VRo values, the pyrolysis T_{\max} values were subsequently used as maturity indicators for the source rocks (e.g., Espitalié 1985). The analyzed Naifa samples have pyrolysis T_{\max} values between 430 and 444 °C (Table 1). These T_{\max} values are generally consistent with the VRo values of 0.64–0.70 and further suggest mature source rock in the early level of oil-generation window (e.g., Peters and Cassa 1994; Hunt 1996).

The thermal maturity level can also be evaluated from PI (Peters and Cassa 1994). In this work, the PI values in the range of 0.01–0.22 are relatively low (Table 1) and indicate that the analyzed samples are in the early stage of oil-generation window, as clearly demonstrated by the relationship between PI and T_{\max} data (Fig. 15).

In addition, a suite of biomarker parameters applied by previous workers (e.g., Seifert and Moldovan 1978, 1981, 1986; Peters et al. 2005) such as CPI, C₃₂-homohopanes 22S/(22S + 22R), moretane to hopane ratio (C_{30M}/C_{30H}), Ts/Tm, and C₂₉ 20S/

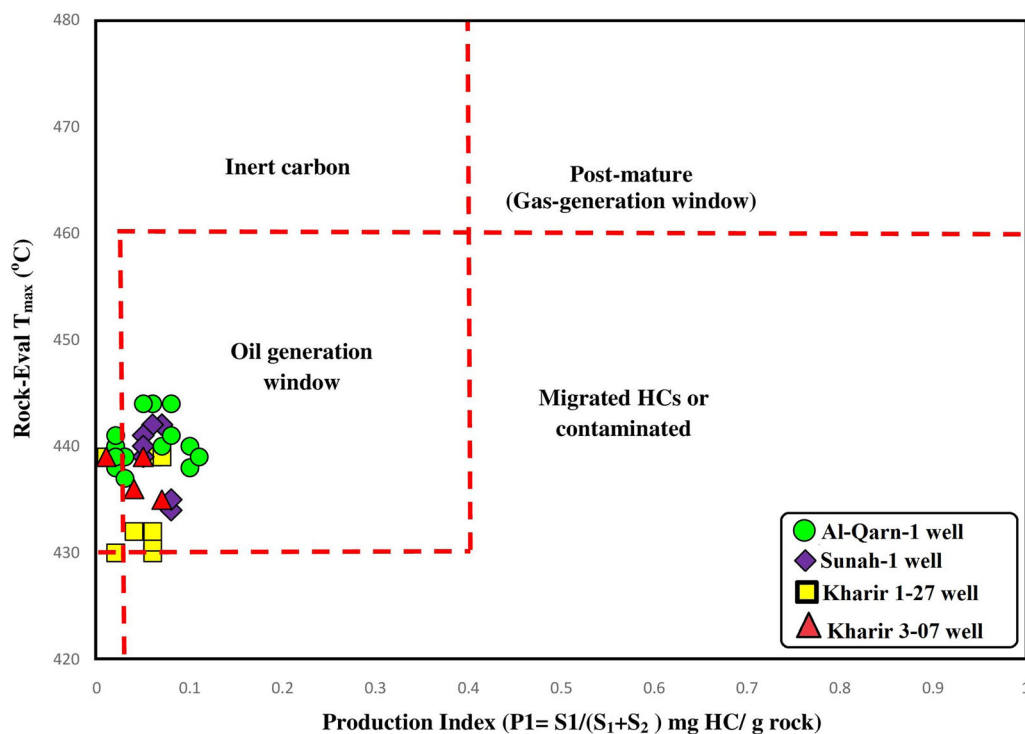


Figure 15. Cross-plots of Rock–Eval pyrolysis T_{\max} vs. PI.

(20S + 20R) and $\beta\beta/(\beta\beta + \alpha\alpha)$ were also calculated (Tables 2 and 4) to evaluate the thermal maturation of the organic matter. The $C_{29} \alpha\alpha\alpha/20S/ (20S + 20R)$ and $C_{29} \beta\beta/(\beta\beta + \alpha\alpha)$ sterane ratios for the 10 analyzed samples are in the range of 0.29–0.38 (Table 4), indicating low-maturity stage (Fig. 16). The relatively high C_{30M}/C_{30H} ratios of the analyzed samples, namely > 0.34 , further indicate that the samples are at low-maturity level (Mackenzie et al. 1980). The C_{32} -hopane ratios are between 0.54 and 0.57, inferring a stage close to the thermal equilibrium for oil-generation window. In accordance with previously obtained maturity data, these results indicate that the analyzed Naifa samples from the studied wells are generally mature source rocks within the early level of oil-generation window.

Hydrocarbon Generation Potential

The characteristics of the kerogen dispersed in potential source rocks will greatly influence the type of the hydrocarbons generated during thermal maturation (Tissot and Welte 1984; Peters and Cassa

1994; Hunt 1996; Katz 2005; Abdullah et al. 2017; Ardakania et al. 2017). This can be evaluated through geochemical and petrological parameters (Tissot and Welte 1984; Hunt 1996). In this study, the quality or type of the organic matter and their relevance to petroleum generation potential in the analyzed samples were determined primarily through geochemical scrutiny of bulk and quantitative pyrolysis data.

Based on the Rock–Eval pyrolysis analysis, the bulk kerogen type present in the analyzed samples is mainly of Types III and II/III with minor amount of Type II (Fig. 4) as determined from their HI values of 50–433 mg HC/g TOC (Table 1). The n -alkyl chain length distribution in the Py–GC attributes indicates that the organic matter in the analyzed samples is mainly of Type III and II/III kerogens (Fig. 5). Furthermore, the biomarker data from the analyzed samples indicate mixed organic matter of marine and terrigenous sources. The palynofacies composition of the analyzed samples also supports mixed kerogen types, with high amounts of terrigenous organic matter such as woody tissue, cuticles (Fig. 5), and sporomorphs in addition to minor marine microfossils such as dinoflagellate cysts

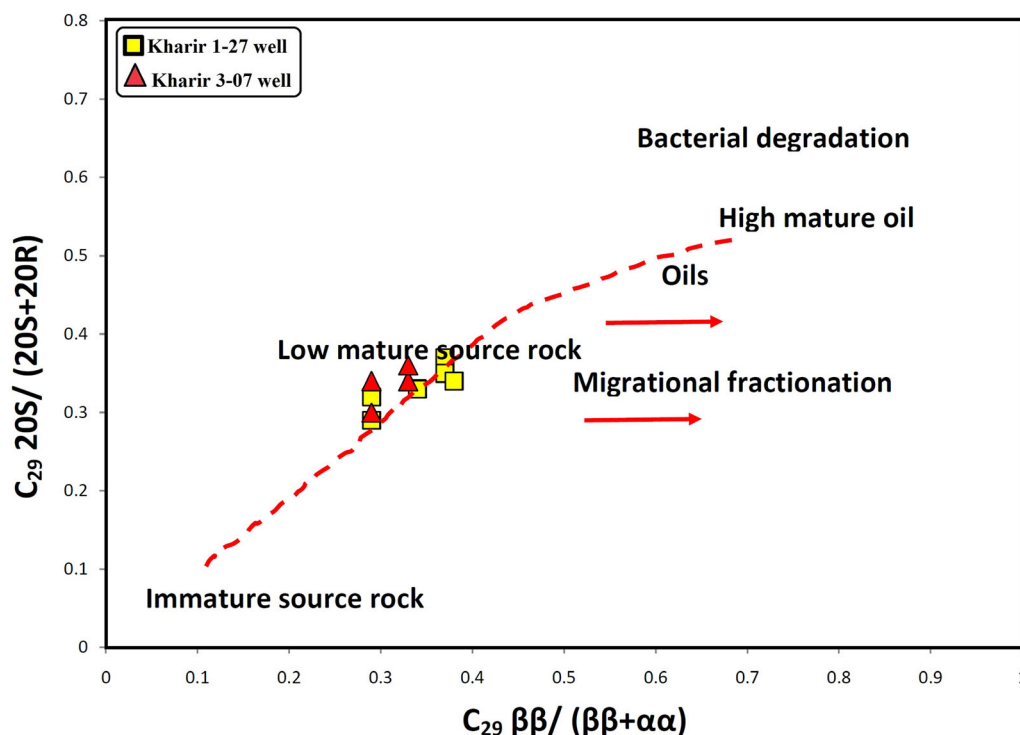


Figure 16. Cross-plot of two biomarker sensitivity parameters (%20S and % $\beta\beta$ sterane) to thermal maturity for the analyzed Naifa samples. Most of the samples plot in the low-maturity source rock fields (after Waples and Machihara 1991).

(Fig. 6). Based on the kerogen type present in this study, the analyzed Naifa Formation samples should be able to generate both oil and gas (Fig. 17) supposing that a sufficient maturity level is reached. The analyzed samples that contained Type II and II/III kerogens indicate potential for generation of oil and gas, whereas those dominated by Type III kerogens imply a mainly gas-prone source rock.

Exploration Implications

According to previous works, hydrocarbon exploration activities in the onshore Say'un–Masila Basin, eastern Yemen, focus primarily on the Late Jurassic Madbi shale source rocks (Mills 1992; Hakimi et al. 2010a; Al Areeq et al. 2011; Hakimi et al. 2012b). Most of the discovered oils are in the organic-rich shales of the Late Jurassic Madbi Formation (Al Areeq and Maky 2015). However, the preliminary results of this study on a relatively younger sequence indicate that the argillaceous limestone intervals within the overlying Late Jurassic–Early Cretaceous Naifa Formation are potential

oil- and gas-prone source rocks, although their relatively low maturity (early oil-window maturity) suggests that they have not yet generated commercial amounts of oil. This important finding will be beneficial for potential prospects and exploration targets in the Say'un–Masila Basin, where the known deeper location of Naifa strata entered the peak oil window and can generate commercial petroleum. Moreover, the source rock characterization of the Naifa Formation, especially with respect organic richness, type of kerogen, maturation and potential of hydrocarbon generation, was discussed for further successful exploration attempts. In this respect, the geochemical properties of the Naifa source rock including TOC, HI, and T_{max} data from the studied wells (Al-Qarn-1, Kharir 1-27, Kharir 3-07, and Sunah-1) were averaged and mapped to show the general lateral distribution throughout the study area (Fig. 18). The lateral distribution shows that the organic matter in terms of TOC% in the Naifa source rock increases from the northwestern area around well Al-Qarn-1 to the central and southeastern parts of the study area particularly in the area around Sunah-1 well (Fig. 18a). The Naifa

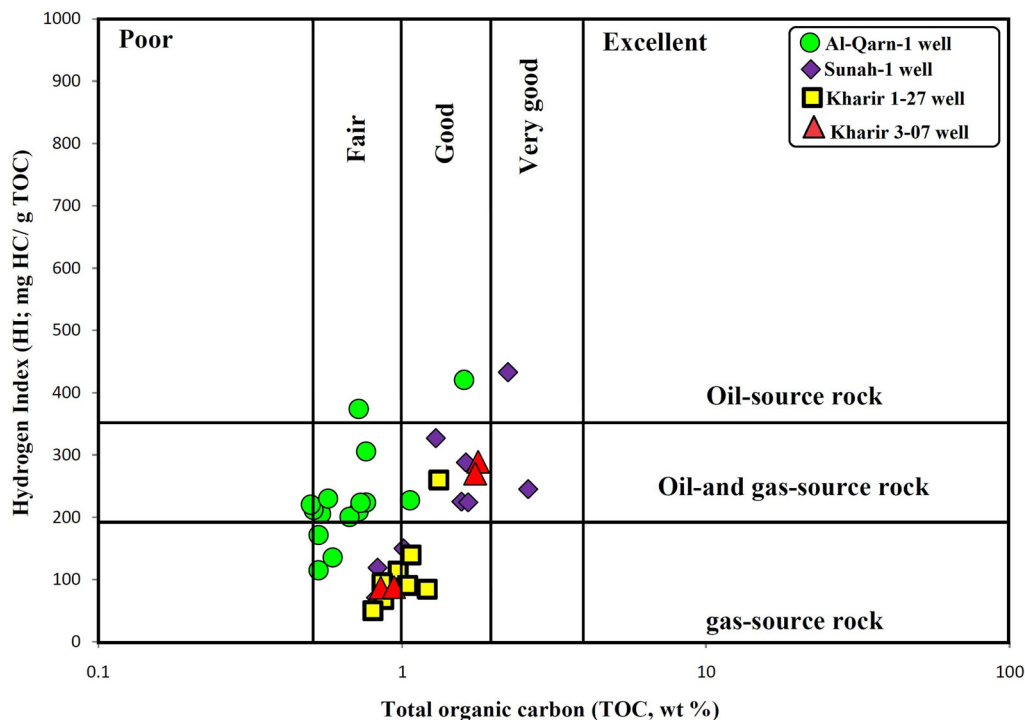


Figure 17. Relationship between TOC and Rock Eval HI.

source rock in the studied wells has HI values in the range of 50–433 mg HC/g TOC (Table 1), and these values increase from the central to the northwestern and southeastern parts particularly in the areas around Al-Qarn-1 and Sunah-1 wells (Fig. 18b). Consequently, the northwestern and southeastern parts have higher oil-generation potential than the central parts. This distribution also suggests that the Naifa source rock unit is more mature in the northwestern part of the study area, followed by the southeastern part as indicated from the geochemical maturity T_{\max} data (Fig. 18c), which can be attributed to the regularly increasing burial depth from the central toward the northwestern and southeastern parts (Fig. 18d).

The distributions of the source rock geochemical results of the Naifa source rock suggest that good source rock properties are recognized in the southeastern part of the study area, which can be considered to have high oil-generation potential corresponding to high TOC and HI values (Fig. 18a and b), and reached a sufficient burial maturity level

(Fig. 18c and d). Therefore, we envisage that the source rock characteristics of the Naifa Formation in the deeper parts of the basin, particularly in the areas around Sunah-1 and Al-Qarn-1 wells, offer guidance for potential prospects and petroleum exploration targets. Moreover, the biomarker parameters and depositional environment indicators presented and discussed in this study are also useful for future exploration in the Say'un–Masila Basin, for oil–oil and oil–source geochemical correlations for future hydrocarbon exploration in the basin.

CONCLUSIONS

Detailed organic geochemical investigation, coupled with palynofacies analysis, was conducted on the late Jurassic–early Cretaceous argillaceous limestone of the Naifa Formation using rock samples gathered from four wells in the Say'un–Masila Rift Basin. The following points summarize the main conclusions of this study.

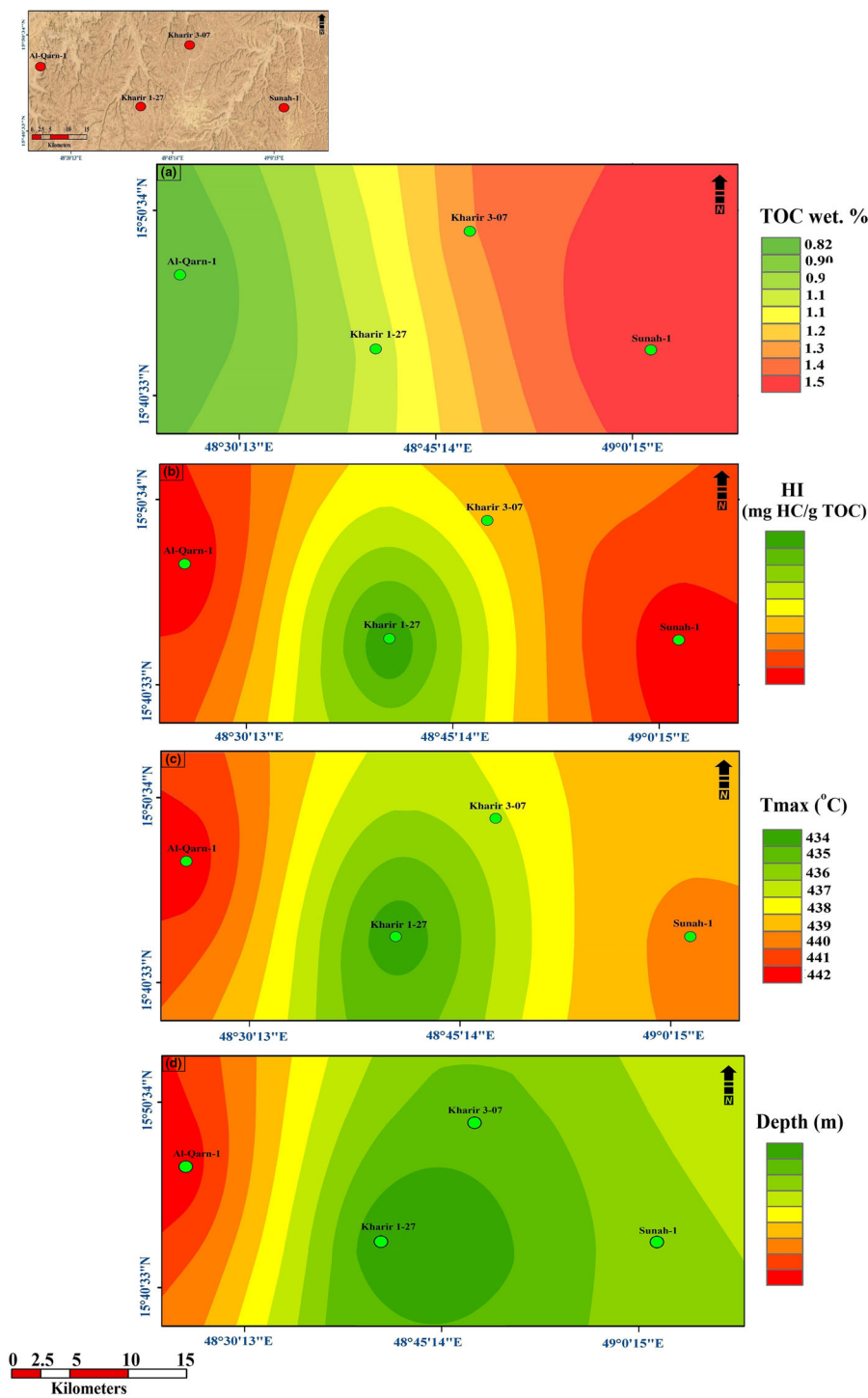


Figure 18. Maps of lateral distributions of the geochemical results, i.e., TOC, HI, and T_{max} (a-c) and the depth of the Naifa Formation (d), showing that most prospective areas are located in the northwestern and southeastern parts, particularly in the areas around Al-Qarn-1 and Sunah-1 wells.

1. The analyzed samples Naifa argillaceous limestone have TOC in the range of 0.50–2.60 wt%, indicating fair to good potential source rocks.
2. The organic matter is predominantly of Type II/III and III kerogens and minor Type II kerogen, with HI in the range of 50–433 mg HC/g TOC. These indicate potential to generate both oil and gas. The characteristics of the Types II/III and III determined based on Py–GC analysis indicate that the Naifa samples contain mixed marine organic matter with significant amounts of terrestrial organic matter input.
3. The biological markers, such as relatively low Pr/Ph ratios of 1.26–1.67 and high C_{31} -22R-hopane/ C_{30} -hopane and C_{29} -norhopane/ C_{30} -hopane ratios, indicate that the analyzed Naifa samples are carbonate-rich and were deposited in a marine setting under sub-oxic conditions. The relatively high CPI and C_{27} and C_{29} regular sterane biomarkers also revealed that the organic matter originated from mixed marine and terrigenous sources. This interpretation is also supported by the abundance of terrestrial-derived materials such as vitrinite phytoclasts, spores, and pollen in addition to minor occurrences of marine microfossils as observed under the microscope.
4. The combination of maturity indicators such as vitrinite reflectance, pyrolysis T_{max} and biomarkers data reveals an oil window maturity equivalent to early-mature level. This indicates that no commercially viable oil or gas has been generated from the areas immediately around the studied wells.
5. Although the analyzed samples recorded low mature level, there is possibility that the Naifa Formation entered the peak oil window and can generate commercial petroleum at deeper burial depths within the basin, particularly in the areas around Sunah-1 and Al-Qarn-1 wells. Therefore, more focus should be given on the known deeper location of Naifa strata for potential prospects and exploration targets.

ACKNOWLEDGMENTS

The Petroleum Exploration and Production Authority (PEPA) and the Total Oil Exploration and Production Company, Republic of Yemen, are acknowledged for providing the data used in the current study. The authors extend their sincere appreciation to the Researchers Supporting Project number (RSP-2019/92), King Saud University, Riyadh, Saudi Arabia. Special thanks go to the Department of Geology, University of Malaya, Malaysia, for providing the use of organic geochemical and petrology facilities to complete this research. The constructive comments by the editor and the anonymous reviewers that improved the original article are gratefully acknowledged.

APPENDIX

See Table 5.

Table 5. Peak assignments for alkane hydrocarbons in the gas chromatograms of saturated fractions in the m/z 191 (I) and 217 (II) mass fragmentograms

Compound abbreviation		
<i>(I) Peak no.</i>		
Ts	18 α (H),22,29,30-trisnorneohopane	Ts
Tm	17 α (H),22,29,30-trisnorhopane	Tm
29	17 α ,21 β (H)-nor-hopane	C_{29} hop
30	17 α ,21 β (H)-hopane	Hopane
3 M	17 β ,21 α (H)-Moretane	C_{30} Mor
31S	17 α ,21 β (H)-homohopane (22S)	C_{31} (22S)
31R	17 α ,21 β (H)-homohopane (22R)	C_{31} (22R)
32S	17 α ,21 β (H)-homohopane (22S)	C_{32} (22S)
32R	17 α ,21 β (H)-homohopane (22R)	C_{32} (22R)
33S	17 α ,21 β (H)-homohopane (22S)	C_{33} (22S)
33R	17 α ,21 β (H)-homohopane (22R)	C_{33} (22R)
34S	17 α ,21 β (H)-homohopane (22S)	C_{34} (22S)
34R	17 α ,21 β (H)-homohopane (22R)	C_{34} (22R)
35S	17 α ,21 β (H)-homohopane (22S)	C_{35} (22S)
35R	17 α ,21 β (H)-homohopane (22R)	C_{35} (22R)
<i>(II) Peak no.</i>		
a	13 β ,17 α (H)-diasteranes 20S	Diasteranes
b	13 β ,17 α (H)-diasteranes 20R	Diasteranes
c	13 α ,17 β (H)-diasteranes 20S	Diasteranes
d	13 α ,17 β (H)-diasteranes 20R	Diasteranes
e	5 α ,14 α (H), 17 α (H)-steranes 20S	$\alpha\alpha$ 20S
f	5 α ,14 β (H), 17 β (H)-steranes 20R	$\alpha\beta$ 20R
g	5 α ,14 β (H), 17 β (H)-steranes 20S	$\alpha\beta$ 20S
h	5 α ,14 α (H), 17 α (H)-steranes 20R	$\alpha\alpha$ 20R

REFERENCES

- Abdullah, W. H. (1999). Oil generating potential of Tertiary coals and other organic-rich sediments of the Nyalau Formation, onshore Sarawak. *Journal of Asian Earth Sciences*, 17, 255–267.
- Abdullah, W. H., Togunwa, O. S., Makeen, Y. M., Hakimi, M. H., Mustapha, K. A., Baharuddin, M. H., et al. (2017). Hydrocarbon source potential of eocene–miocene sequence of Western Sabah, Malaysia. *Marine and Petroleum Geology*, 83, 345–361.
- Adegoke, A. K., Abdullah, W. H., & Hakimi, M. H. (2015). Geochemical and petrographic characterisation of organic matter from the Upper Cretaceous Fika shale succession in the Chad (Bornu) Basin, northeastern Nigeria: Origin and hydrocarbon generation potential. *Marine and Petroleum Geology*, 61, 95–110.
- Adegoke, A. K., Abdullah, W. H., & Yandoka, B. M. S. (2017). Provenance and paleoenvironment of organic matter within the Fika sediments in Chad (Bornu) Basin, northeastern Nigeria: An integrated organic geochemical and palynofacies approach. *International Journal of Coal Geology*, 173(C), 94–109.
- Al Areeq, N. A., & Al-Auge, A. S. (2014). Well log analysis and hydrocarbon potential of the Sa'ar–Nayfa reservoir, Hiswah Oilfield, eastern Yemen. *Arabian Journal Geosciences*. <http://doi.org/10.1007/s12517-013-1003-5>.
- Al Areeq, N. A., & Maky, A. F. (2015). Organic geochemical characteristics of crude oils and oil-source rock correlation in the Sunah oilfield, Masila Region, Eastern Yemen. *Marine and Petroleum Geology*, 63, 17–27.
- Al Areeq, N. M., Soliman, M. A., Essa, M. A., & Al-Azazi, N. A. (2015). Diagenesis and reservoir quality analysis in the Lower Cretaceous Qishn sandstones from Masila oilfields in the Sayun–Masila Basin, eastern Yemen. *Geological Journal*.
- Al-Areeq, N. M., Abu El Ata, A. S., Maky, A. F., & Omran, A. A. (2011). Hydrocarbon Potentialities of some upper jurassic rock units in Masila Block, Sayun-Masila basin, Yemen. National Research Center, Cairo. *Journal of Applied Geophysics*, 10, 147–168.
- Alias, F. L., Abdullah, W. H., Hakimi, M. H., Azhar, M. H., & Kugler, R. L. (2012). Organic geochemical characteristics and depositional environment of the Tertiary Tanjong Formation coals in the Pinangah area, onshore Sabah, Malaysia. *International Journal of Coal Geology*, 104, 9–21.
- Al-Wosabi, M. A., & Al-Mashaikie, S. Z. (2006). Investigation of facies types and associations of Kuhlan Red Bed Formation in NW Yemen: A new hypothesis for origin and depositional environment. *SQU Journal for Science*, 11, 11–38.
- Ardakania, O. M., Saneia, H., Ghanizadeh, A., McMechan, M., Ferric, F., & Clarkson, C. (2017). Hydrocarbon potential and reservoir characteristics of lower Cretaceous Garbutt Formation, Liard Basin Canada. *Fuel*, 209, 274–289.
- Batten, D. J., & Stead, D. T. (2005). Palynofacies analysis and its stratigraphic application. In E. A. M. Koutsoukos (Ed.), *Applied stratigraphy* (pp. 203–226). Amsterdam: Springer.
- Bawazer, W., Lashin, A., & Kinawy, M. M. (2018). Characterization of a fractured basement reservoir using high-resolution 3D seismic and logging datasets: A case study of the Sab'atayn Basin, Yemen. *PLoS ONE*, 13(10), e0206079.
- Beydoun, Z. R. (1964). The stratigraphy and structure of the eastern Aden Protectorate. In *Overseas geological and mineral resources* (Bull. Supp. 5, pp. 1–107). London: HMSO.
- Beydoun, Z. R., Al-Saruri, M., El-Nakhal, H., Al-Ganad, I. N., Baraba, R. S., Nani, A. S. O., et al. (1998). *International lexicon of stratigraphy*, V. III, Republic of Yemen, Second Ed. International Union of Geological Sciences and Ministry of Oil and Mineral Resources, Republic of Yemen, Publication 34, 245 p.
- Chandra, K., Mishra, C. S., Samanta, U., Gupta, A., & Mehrotra, K. L. (1994). Correlation of different maturity parameters in the Ahmedabad–Mehsana Block of the Cambay Basin. *Organic Geochemistry*, 21, 313–321.
- Colombo, J. C., Pelletier, E., Brochu, C., Khalil, M., & Catoggio, J. A. (1989). Determination of hydrocarbon sources using *n*-alkane and polyaromatic hydrocarbon distribution indexes. Case study: Rio de La Plata estuary, Argentina. *Environmental Science & Technology*, 23, 888–894.
- Csato, I., Habib, A., Kiss, K., Kocz, I., Kovacs, V., Lorincz, K., et al. (2001). Play concepts of oil exploration in Yemen. *Oil Gas Journal*, 99(23), 68–74.
- Dembicki, H. J. (2009). Three common source rock evaluation errors made by geologists during prospect or play appraisals. *AAPG*, 93(3), 341–356.
- Dembicki, H., Jr., Horsfield, H. B., & Ho, T. T. Y. (1983). Source rock evaluation by pyrolysis-gas chromatography. *AAPG*, 67, 1094–1103.
- Didyk, B. M., Simoneit, B. R. T., Brassell, S. C., & Eglinton, G. (1978). Organic geochemical indicators of palaeoenvironmental conditions of sedimentation. *Nature*, 272, 216–222.
- Durand, B., & Monin, J. C. (1980). Elemental analysis of kerogens (C, H, O, N, S, Fe). In B. Durand (Ed.), *kerogen* (pp. 113–142). Paris: Editions Technip.
- Escobar, M., M'arquez, G., Inciarte, S., Rojas, J., Esteves, I., & Malandrino, G. (2011). The organic geochemistry of oil seeps from the Sierra de Perij'a eastern foothills, Lake Maracaibo Basin, Venezuela. *Organic Geochemistry*, 42, 727–738.
- Espitalié, J. (1985). Use of T_{max} as a maturation index for different types of organic matter-comparison with vitrinite reflectance. In J. Burrus (Ed.), *Thermal modeling in sedimentary basins* (pp. 475–496). Paris: Editions Technip.
- Espitalié, J. L., Laporte, M., Madec, F., Marquis, P., & Leplat, J. P. (1977). Method rapide de caracterisation des roches meres, de leur potentiel petrolier et de leur degre d'evolution. *Rev. Institute French of Petroleum*, 32, 23–42.
- Farhaduzzaman, M., Abdullah, W. H., & Islam, M. A. (2012). Depositional environment and hydrocarbon source potential of the Permian Gondwana coals from the Barapukuria Basin, Northwest Bangladesh. *International Journal of Coal Geology*, 90(91), 162–179.
- Hakimi, M. H., Abdullah, W. H., Alias, F. L., Azhar, M. H., & Makeen, Y. M. (2013). Organic petrographic characteristics of Tertiary (Oligocene–Miocene) coals from eastern Malaysia: Rank and evidence for petroleum generation. *Internal Journal of Coal Geology*, 20, 71–81.
- Hakimi, M. H., Abdullah, W. H., & Shalaby, M. R. (2010a). Source rock characterization and oil generating potential of the Jurassic Madbi Formation, onshore East Shabawah oilfields, Republic of Yemen. *Organic Geochemistry*, 41, 513–521.
- Hakimi, M. H., Abdullah, W. H., & Shalaby, M. R. (2010b). Organic geochemistry, burial history and hydrocarbon generation modeling of the Upper Jurassic Madbi Formation, Masila Basin, Yemen. *Journal of Petroleum Geology*, 33, 299–318.
- Hakimi, M. H., Abdullah, W. H., & Shalaby, M. R. (2011). Organic geochemical characteristics and depositional environments of the Jurassic shales in the Masila Basin of Eastern Yemen. *GeoArabia*, 16, 47–64.
- Hakimi, M. H., Abdullah, W. H., & Shalaby, M. R. (2012a). Geochemical and petrographic characterization of organic matter in the Upper Jurassic Madbi shale succession (Masila Basin, Yemen): Origin, type and preservation. *Organic Geochemistry*, 49, 18–29.
- Hakimi, M. H., Al-Qadasi, B. A., Al-Sorore, O.T., Al-Sharrabi, Y., & Al-Samet, N. G., (2016). Petrophysical properties of

- Cretaceous clastic rocks (Qishn formation) in the Sharyoof oilfield, onshore Masila Basin, Yemen. *Egyptian Journal of Petroleum* (In press).
- Hakimi, M. H., Shalaby, M. R., & Abdullah, W. H. (2012b). Diagenetic characteristics and reservoir quality of the Lower Cretaceous Biyadh sandstones at Kharir oilfield in the western central Masila Basin, Yemen. *Journal Asian Earth Sciences*, *51*, 109–120.
- Harry, D. J. (2008). Three common source rock evaluation errors made by geologists during prospect or play appraisals. *AAPG*, *93*, 4341–4356.
- Horsfield, B. (1989). Practical criteria for classifying kerogens: Some observations from pyrolysis–gas chromatography. *Geochimica et Cosmochimica Acta*, *53*, 891–901.
- Horsfield, B. (1997). The bulk composition of first-formed petroleum in source rocks. In D. H. Welte, B. Horsfield, & D. R. Backer (Eds.), *Petroleum and basin evolution; insights from petroleum geochemistry, geology and basin modeling*. Berlin: Springer.
- Horsfield, B., & Dueppenbecker, S. (1991). The decomposition of Posidonia Shale and Green River Shale kerogens using micro-scale sealed vessel (MSSV) pyrolysis. *Journal of Analytical and Applied Pyrolysis*, *20*, 107–123.
- Huang, W. Y., & Meinschein, W. G. (1979). Sterols as ecological indicators. *Geochimica et Cosmochimica Acta*, *43*, 739–745.
- Huang, W. B., Salad Hersi, O., Lu, S. F., & Deng, S. W. (2017). Quantitative modelling of hydrocarbon expulsion and quality grading of tight oil lacustrine source rocks: Case study of Qingshankou 1 member, central depression, Southern Songliao Basin, China. *Marine and Petroleum Geology*, *84*, 34–48.
- Hunt, J. M. (1996). *Petroleum geochemistry and geology*. New York: W.H. Freeman and Company.
- Katz, B.J. (2005). Controlling factors on source rock development—a review of productivity, preservation and sedimentation rate. In N. B. Harris (Ed.), *The depositional of organic-carbon-rich rocks: models, mechanisms and consequences* (Vol. 82, pp. 7–16). SEPM Special Publication.
- Khamis, M., Marta, E. B., Al Natifi, A., Fattah, K. A., & Lashin, A. (2017). Simulation of the multi zones clastic reservoir: A case study of Upper Qishn clastic member, Masila Basin-Yemen. *Journal African Earth Sciences*, *130*, 252–268.
- King, W. A., Mills, B. R., Gardiner, S., & Abdillan, A. A. (2003). The Masila fields, Republic of Yemen. In M. T. Halbouty (Ed.), *Giant oil and gas fields of the decade 1990–1999*. AAPG memories (Vol. 78, pp. 275–295).
- Larter, S. R. (1984). Application of analytical pyrolysis technique to kerogen characterization and fossil fuel exploitation. In K. Voorhees (Ed.), *Analytical pyrolysis* (pp. 212–275). London: Butterworth.
- Lashin, A., Marta, E. B., & Khamis, M. (2016). Characterization of the Qishn sandstone reservoir, Masila Basin-Yemen, using an integrated petrophysical and seismic structural approach. *Journal African Earth Sciences*, *115*, 121–142.
- Mackenzie, A. S., Patience, R. L., Maxwell, J. R., Vandembroucke, M., & Durand, B. (1980). Molecular parameters of maturation in the Toarcian shales, Paris Basin, France. Changes in the configuration of acyclic isoprenoids alkanes, steranes and triterpanes. *Geochimica et Cosmochimica Acta*, *44*, 1709–1721.
- Makeen, Y. M., Abdullah, W. H., & Hakimi, M. H. (2015). Biological markers and organic petrology study of organic matter in the Lower Cretaceous Abu Gabra sediments (Muglad Basin, Sudan): Origin, type and palaeoenvironmental conditions. *Arabian Journal Geosciences*, *8*, 489–506.
- Manning, D. A. C. (1991). *Organic geochemistry: Advances and applications in the natural environment*. Manchester, UK: Manchester University Press.
- Mills, S. J. (1992). Oil discoveries in the Hadramaut: How Canadian oxy scored in Yemen. *Oil Gas Journal*, *49*, 52.
- Mohialdeen, I. M. J., & Hakimi, M. H. (2016). Geochemical characterisation of Tithonian–Berriasian Chia Gara organic-rich rocks in northern Iraq with an emphasis on organic matter enrichment and the relationship to the bioproductivity and anoxia conditions. *Journal of Asian Earth Sciences*, *116*, 181–197.
- Moldowan, J. M., Sundaraman, P., & Schoell, M. (1986). Sensitivity of biomarker properties to depositional environment and/or source input in the Lower Toarcian of S.W, Germany. *Organic Geochemistry*, *10*, 915–926.
- Nøhr-Hansen, H. (1989). Visual and chemical kerogen analyses of the Lower Kimmeridgian Clay, Westbury, England. In D. J. Batten & M. C. Keen (Eds.), *Northwest European micropalaeontology and palynology* (pp. 118–132). Chichester: Ellis Horwood Limited.
- Peters, K. E., & Cassa, M. R. (1994). *Applied source rock geochemistry*. In L. B. Magoon & W. G. Dow (Eds.), *The petroleum system—from source to trap*. AAPG memories (Vol. 60, pp. 93–120).
- Peters, K. E., & Moldowan, J. M. (1993). *The biomarker guide: Interpreting molecular fossils, petroleum and ancient sediments* (p. 363). New Jersey: Prentice Hall.
- Peters, K. E., Walters, C. C., & Moldowan, J. M. (2005). *The biomarker guide* (p. 1155). UK: Cambridge University Press.
- Ramanampisoa, L., Radke, M., Schaeffer, G., Littke, R., Rullkötter, J., & Horsfield, B. (1990). Organic-geochemical characterisation of sediments from the Sakoa coalfield, Madagascar. *Organic Geochemistry*, *16*, 235–246.
- Redfern, P., & Jones, J. A. (1995). The interior basins of Yemen—analysis of basin structure and stratigraphy in a regional plate tectonic context. *Basin Research*, *7*, 337–356.
- Robinson, K. J. (1987). An overview of source rocks and oils in Indonesia. In *Proceedings of the Indonesian Petroleum Association, 16th annual convention, V I. Indonesian Petroleum Association, Jakarta* (pp. 97–122).
- Sarki Yandoka, B. M., Abubakar, M. B., Abdullah, W. H., Hakimi, M. H., & Adegoke, A. K. (2015a). Geochemistry of the Cretaceous coals from Lamja Formation, Yola Sub-basin, Northern Benue Trough, NE Nigeria: Implications for paleoenvironment, paleoclimate and tectonic setting. *Journal of African Earth Sciences*, *104*, 56–70.
- Sarki Yandoka, B. M., Abubakar, M. B., Abdullah, W. H., Hakimi, M. H., & Adegoke, A. K. (2015b). Geochemical characterisation of Early Cretaceous lacustrine sediments of Bima Formation, Yola Sub-basin, Northern Benue Trough, NE Nigeria: Organic matter input, preservation, paleoenvironment and paleoclimatic conditions. *Marine and Petroleum Geology*, *61*, 82–94.
- Seifert, W. K., & Moldowan, J. M. (1978). Applications of steranes, terpanes and monoaromatics to the maturation, migration and source of crude oils. *Geochimica et Cosmochimica Acta*, *42*, 77–95.
- Seifert, W. K., & Moldowan, J. M. (1981). Palaeoreconstruction by biological markers. *Geochimica et Cosmochimica Acta*, *45*, 783–794.
- Seifert, W. K., & Moldowan, J. M. (1986). *Use of biological markers in petroleum exploration*. In R. B. Johns (Ed.), *Methods in geochemistry and geophysics book series* (Vol. 24, pp. 261–90). Amsterdam.
- SPT. (1994). *The petroleum geology of the sedimentary basins of the republic of Yemen, V. 1e7* (unpublished report).
- Staplin, F. L. (1982). Determination of thermal alteration index from color of exinite (pollen, spores). In F.L. Staplin (Ed.), *How to assess maturation and paleotemperatures*. SEPM short course (Vol. 7, pp. 7–11).

- Sweeney, J. J., & Burnham, A. K. (1990). Evaluation of a simple model of vitrinite reflectance based on chemical kinetics. *AAPG*, 74, 1559–1570.
- Teichmüller, M. (1958). *Metamorphism du carbon et projection du pétrole* (pp. 1–15). Special Issue: Review of Industrial Minerals.
- Tissot, B. T., & Welte, D. H. (1984). *Petroleum formation and occurrences* (2nd ed.). Berlin: Springer.
- Togunwa, O. S., Abdullah, W. H., Hakimi, M. H., & Barbeitoc, P. J. (2015). Organic geochemical and petrographic characteristics of Neogene organic-rich sediments from the onshore West Baram Delta Province, Sarawak Basin: Implications for source rocks and hydrocarbon generation potential. *Marine and Petroleum Geology*, 63, 115–126.
- Tyson, R. V. (1995). *Sedimentary organic matter: Organic facies and palynofacies* (p. 615). London: Chapman and Hall.
- Waples, D. W., & Machihara T. (1991). Biomarkers for Geologists: A practical guide to the application of steranes and triterpanes in petroleum geology. In *AAPG methods in exploration series*, 9, Tulsa, Oklahoma.